UNIVERSITEIT VAN PRETORIA
UNIVERSITY OF PRETORIA
YUNIBESITHI YA PRETORIA

Geochemistry and spatial variation in dolerites of the Drakensberg Group, Karoo Supergroup, South Africa

Arnoldus Daniel Kotze

04541686

Department of Geology

University of Pretoria

Abstract

The Karoo Large Igneous Province (KLIP) in South Africa comprises a spatially limited basalt suite (Drakensberg Group) and a spatially extensive dolerite suite. This study aims to establish a tectonic regime that could have facilitated the KLIP and the extent of geochemical variation in the dolerite suite. Principal component analysis (PCA) is used to identify trends as this multivariate statistical operation is particularly well suited to identifying possible petrological processes. Major and trace element chemistry is interpreted from data made available by GeoROC, a public geochemical data depository. This study observed 139 samples of which 49 were basalts and 90 were dolerites, sampled along a c. 1500 km E-W tract along the southern margins of the Karoo basin. Disassociations between the KLIP and surficial manifestations of mantle plumes are discussed. Transition metal chemistry is described using Co, Cr, Cu, Ni, V, and Zn; however, anomalies in the transition metal data resulted in only LILs (Ba, Sr, and Rb) and HFSEs (Nb and Zr, and the REEs Ce, La, Nd, and Y) being used to investigate spatial variation in the KLIP. Spatial variation could not be inferred with major element chemistry nor with trace element chemistry, and the data is remarkably compatible to the lower crust. Although it is suggested that gravity could have been a driving force behind the KLIP, further studies must be done to provide a better understanding of the relationships between the KLIP and its host geology.

DECLARATION OF ORIGINALITY / DECLARATION ON PLAGIARISM

The ***Department of Geology (University of Pretoria)*** places great emphasis upon integrity and ethical conduct in the preparation of all written work submitted for academic evaluation. While academic staff teaches you about referencing techniques and how to avoid plagiarism, you too have a responsibility in this regard. If you are at any stage uncertain as to what is required, you should speak to your lecturer before any written work is submitted.

You are guilty of plagiarism if you copy something from another author's work (e.g. a book, an article or a website) without acknowledging the source and pass it off as your own. In effect, you are stealing something that belongs to someone else. This is not only the case when you copy work word-for-word (verbatim), but also when you submit someone else's work in a slightly altered form (paraphrase) or use a line of argument without acknowledging it. You are not allowed to use work previously produced by another student. You are also not allowed to let anybody copy your work with the intention of passing if off as his/her work.

Students who commit plagiarism will not be given any credit for plagiarised work. The matter may also be referred to the Disciplinary Committee (Students) for a ruling. Plagiarism is regarded as a serious contravention of the University's rules and can lead to expulsion from the University.

The declaration which follows must accompany all written work submitted while you are a student of the ***Department of Geology (University of Pretoria)***. No written work will be accepted unless the declaration has been completed and attached.

- I, the undersigned, declare that:
- I understand what plagiarism is and am aware of the University's policy in this regard.
- I declare that this assignment (e.g. essay, report, project, assignment, dissertation, thesis, etc.) is my own original work. Where other people's work has been used (either from a printed source, Internet or any other source), this has been properly acknowledged and referenced in accordance with Departmental requirements.
- I have not used work previously produced by another student or any other person to hand in as my own.
- I have not allowed, and will not allow, anyone to copy my work with the intention of passing it off as his or her own work.

Full names of student: _____

Student number: _____

Date submitted: _____

Topic of work: _____

Signature: _____

Supervisor: _____

Table of Contents

List of Figures iv

List of Tables vii

Introduction 1

Background 6

The Karoo Supergroup 6

The Karoo basin 9

The Karoo ring-dyke complexes 11

Broad geochemical overview Karoo dolerite 12

The Karoo mantle plume 13

Other work done with principal component analysis 14

Methodology 16

Data description 16

Data processing 18

Results 20

Major element chemistry 20

Transition element chemistry 23

LIL and HFSE behaviour 27

Discussion 33

Representability of the study 33

Implications of the findings 34

The Karoo LIP as it stands now 36

Karoo basin geodynamic environment 37

The plume model for the Karoo 40

A model for intraplate magmatism 41

Conclusion 44

Works Cited 45

List of Figures

Figure 1: Seemingly random distribution of dolerite dykes in the Main Karoo basin. The assumption is made that all of these structures are Karoo dykes (i.e. dolerite and c. 180 Ma in age) (Chevallier & Woodford, 1999). 2

Figure 2: Map showing the Karoo Large Igneous Province (KLIP) in red and the famed Karoo Triple Junction in blue. The map depicts the prevalent tectonic regime at the time. The insert inadvertently places an emphasis on understanding how the geochemistry of the KLIP fits into the narrative of the break-up of southern Gondwana. Southern Karoo CFBs are depleted in Nb relative to Northern Karoo CFBs. The spatially limited suite basaltic suite (Drakensberg Group) is inferred form the continuous red mass labelled "Lesotho". Taken from Luttinen (2018). 2

Figure 3: The top diagram (3a) shows the Karoo data in the TAS system of Cox et al. (1979). Triangles denote extrusive data and circles denote intrusive data. Grey triangles are Lesotho basalt Group 1 and purple triangles are Lesotho basalt Group 2. Intrusive data comprises data from several locations; Karoo Central Area (KCA; yellow), Golden Valley Sill complex (GVS; blue), KWV Sill (KWV; red) and Underberg Dyke Swarm (UDS; green). Figure 3b (bottom) shows the Karoo data (blue) relative to data from the Siberian (red) and Deccan (green) flood basalt provinces. 4

Figure 5: Map showing the outcrops of the Karoo Supergroup. Taken from Johnson et al. (1997). The red rectangle shows an approximation where Figure 6 can be found on this map. 7

Figure 4: A cross section of the Karoo basin. Pre-Cape rocks refers to the basement rocks of the Namaqua-Natal Metamorphic Province. Taken from Johnson et al., (1997). Main Karoo basin refers to the Karoo basin as there are other Karoo-aged basins in southern Africa ((Catuneanu, et al., 2005). 7

Figure 6: Drakensberg Group flood basalts are shown in red. The location of the Sterkspruit Complex is indicated. Modified from McClintock et al. (2002). 8

Figure 7: Diagram showing the flexural mechanics at work in a conventional retro-arc foreland basin. The symbol λ is used to show flexural wavelength. Flexing is attributed towards orogenic loading. Modified from Catuneanu (2004). 9

Figure 8: Bouguer gravity anomalies showing the crustal structure of South Africa underlying the Main Karoo basin. BF: Brakbos fault; BRT: Blackridge thrust; CDL: Commondale lineament; Ca: Cango Caves Group; Co: Colenso fault; G: George; Ga: Gamtoos Group; Gr: Gariep Group; GT: Groothoek thrust; Ka: Kaaimens Group; KF: Kalahari fault; KHF: Kheis fault; L: Letseng-la-Tarae kimberlite; LML: Lilani-Matigulu lineament; M: Matsoku kimberlite; Mb: Malmesbury Group; MT: Melville thrust; Na: Nama Group; TTF: Tugela thrust front. Modified from Tankard et al. (2009). 10

Figure 10 (right): A map of the Golden Valley Sill Complex. Here the general structural configuration of the ring-dyke complexes may be observed well. GVS, Golden Valley Sill; GS, Glen Sill; HS, Harmony Sill; MS, Morning Sun Sill; L1, L1 sill; GVD, Golden Valley Dyke (Neumann, et al., 2011). 11

Figure 9 (top): Thin-skinned Jura-type fold belt model for the Cape Fold Belt. Vertical movement is recognized but attributed towards flexural mechanics in contrast to subsidence as in Tankard et al.

(2009). . NNMP refers to the Namaqua-Natal Metamorphic Belt. Modified from Lindeque et al. (2011). 11
Figure 11: (right) Three component system responsible for the formation of ring-dyke complexes according to Chevalier and Woodford (1999). 12
Figure 12: 12
Figure 13: Neumann et al.'s (2011) model for the petrogenisis of the dolerites in the Karoo basin. 13
Figure 14: Map showing the sampling locations of data used in this study. Sampling of intrusive material occurred in, and moving from left to right, 1) the Karoo Central area (KCA), 2) Golden Valley Sill complex (GVS), 4) KWV sill, and 3) Underberg Dyke Swarm (UDS). Extrusive material is divided into a 5) southern and 6) northern group of basalts (LB1 and LB2, respectively) based on relative K and Na contents (Google Earth, 2020). 17
Figure 15: Close up of the spread in data from Figure 3a. Triangles denote extrusive data and circles denote intrusive data. Grey triangles are Lesotho basalt Group 1 and purple triangles are Lesotho basalt Group 2. Intrusive data comprises data from several locations; Karoo Central Area (KCA; yellow), Golden Valley Sill complex (GVS; blue), KWV Sill (KWV; red) and Underberg Dyke Swarm (UDS; green). 20
Figure 16: Harker diagrams of major element chemistry measured against an increase in SiO_2 content. Triangles denote extrusive data and circles denote intrusive data. Grey triangles are Lesotho basalt Group 1 and purple triangles are Lesotho basalt Group 2. Intrusive data comprises data from several locations; Karoo Central Area (KCA; yellow), Golden Valley Sill complex (GVS; blue), KWV Sill (KWV; red) and Underberg Dyke Swarm (UDS; green). 21
Figure 17: Binaries of FeOt and TiO_2 relative to SiO_2. The UDS data mimics the behaviour of GVS data rather than Group 1 basalts and KWV data is more conformable to LB1 basalts than to GVS data. The separation between LB1 and LB2 basalts is apparent in both binaries. 22
Figure 18: The top figure (18a) is the PCA of the transition metals Co, Cu, Cr, Ni, V, and Zn. The bottom figure (18b) shows the data as eigenvalues in a space defined by the two principal components. Data shown are GVS and KWV dolerites (blue and red circles, respectively), and Group 1 Lesotho basalts (grey triangles). A large degree of overlap between the dolerites and basalts may be observed. The GVS data and the KWV data overlap with each other 25
Figure 19: The top figure (19a) is a combined PCA of HFSEs (Nd and Zr) and LILs (Ba, Rb, and Sr). The bottom figure (19b) shows the data as eigenvalues in a space defined by the two principal components. Data shown are GVS and KWV dolerites (blue and red circles, respectively), and Group 1 Lesotho basalts (grey triangles). As with Figure 15 a large degree of overlap between the dolerites and basalts may be observed. The KWV data is not conformable to the rest of the data in 17b in contrast to Figure 15b where the KWV appears to be very conformable to one of the GVS clusters. 28
Figure 20: The top figure (20a) is a PCA of the REEs Ce, La, Nd, and Y. The bottom figure (20b) shows the data as eigenvalues in a space defined by the two principal components. Data shown are GVS and KWV dolerites (blue and red circles, respectively), and Group 1 Lesotho basalts (grey triangles). As with Figure 15, a large degree of overlap between the dolerites and basalts may be observed. 30

Figure 21: Spider plot normalized to the lower continental crust (21a; left) and upper continental crust (21b; right) after Taylor and McLennan (1995). Data shown are Karoo Central Area (KCA; yellow), Golden Valley Sill complex (GVS; blue), KWV Sill (KWV; red), and Underberg Dyke Swarm (UDS; green). The data is far more conformable to the lower continental crust than to the upper continental crust and is depleted relative to the upper continental crust. 32

Figure 22: A PCA of mafic material sampled from a variety of tectonic settings shown as eigenvalues in a space defined by the two principal components. 34

Figure 23: Map and inserts showing the location of Mt Peaktu (Tang, et al., 2011). 42

List of Tables

Table 1: Principal component analysis of the transition metals Co, Cu, Cr, Ni, V, and Zn. The importance of the components may be inferred from the proportion of variance. Generated with GCDkit. 26

Table 2: Results table of the principal component analysis of the transition metals Co, Cu, Cr, Ni, V, and Zn. Generated with R and rounded to four significant figures. Empty cells denote negligible loadings (Everitt & Hothorn, 2011). 26

Table 3: Principal component analysis of the transition metals Co, Cu, Cr, Ni, V, and Zn. The importance of the components may be inferred from the proportion of variance. Generated with GCDkit. 29

Table 4: Results table of the principal component analysis of HFSEs (Nd and Zr) and LILs (Ba, Rb, and Sr). Generated with R and rounded to four significant figures. Empty cells denote negligible loadings (Everitt & Hothorn, 2011). 29

Table 5: Principal component analysis of the REEs Ce, La, Nd, and Y. The importance of the components may be inferred from the proportion of variance. Generated with GCDkit. 31

Table 6: Results table of the principal component analysis of the REEs Ce, La, Nd, and Y. Generated with R and rounded to four significant figures. Empty cells denote negligible loadings (Everitt & Hothorn, 2011). 31

Introduction

The Karoo Large Igneous Province (KLIP) in South Africa comprises a spatially limited basalt suite (Drakensberg Group) and a spatially extensive dolerite suite within the Karoo basin (Fig. 1). The KLIP has been considered a product of plume magmatism (e.g. White, 1997), but some aspects of the magmatism remain unexplained, and a review of Karoo volcanic data necessitates a re-examination of the magmatism. Although Coffin and Eldholm (1992) recognized the KLIP as a Large Igneous Province (LIP), there is no set definition for a LIP. Contemporary understanding of LIPs describes mafic volcanic provinces that were emplaced in less than 5 m.y., had a surface area greater than $1x10^5$ km^2, and volume greater than $1x10^5$ km^3 (Svensen, et al., 2019).

Association between the extrusive and intrusive suites has long been made (e.g. Duncan, 1987; Hastie, et al., 2014; Svensen, et al., 2018) and so the term “Drakensberg Group” is commonly used and includes both suites. The Drakensberg Group is a large constituent of the c. 180 Ma KLIP (Fig. 1) and consequentially forms part of the narrative of the coeval break-up of southern Gondwana (Sweeney & Watkeys, 1990; Ramluckan, 1992; Duncan, et al., 1997; Hawkesworth, et al., 1999). The focal point of this study is two questions pertaining to the spatially extensive dolerite suite. Firstly, what kind of crustal emplacement mechanism (i.e. stress regime) could have facilitated the intrusion of the dolerites? And secondly, what is the extent of variation in the geochemistry of dolerites in the Karoo basin?

Determining the stress regime that could have produced the distribution of the dykes in the Karoo basin (Fig. 2) is an important objective and is more complex than it may appear at first glance. There are global localities where the orientation of linear and sub-linear intrusive bodies can readily be used to determine the prevailing structural controls in an area. For instance, the Great Dyke, a NNE-SSW trending ultramafic structure in Zimbabwe, southern Africa, implies a NNE-SSW directed pressure in the area (Schoenberg, et al., 2003) and the intrusion expanded accordingly; i.e. orthogonal to the direction of highest compressive force. In the Karoo basin, however, there is simply not enough consistent evidence to identify a general trend in the spatial distribution of the Karoo dyke (Chevallier & Woodford, 1999).

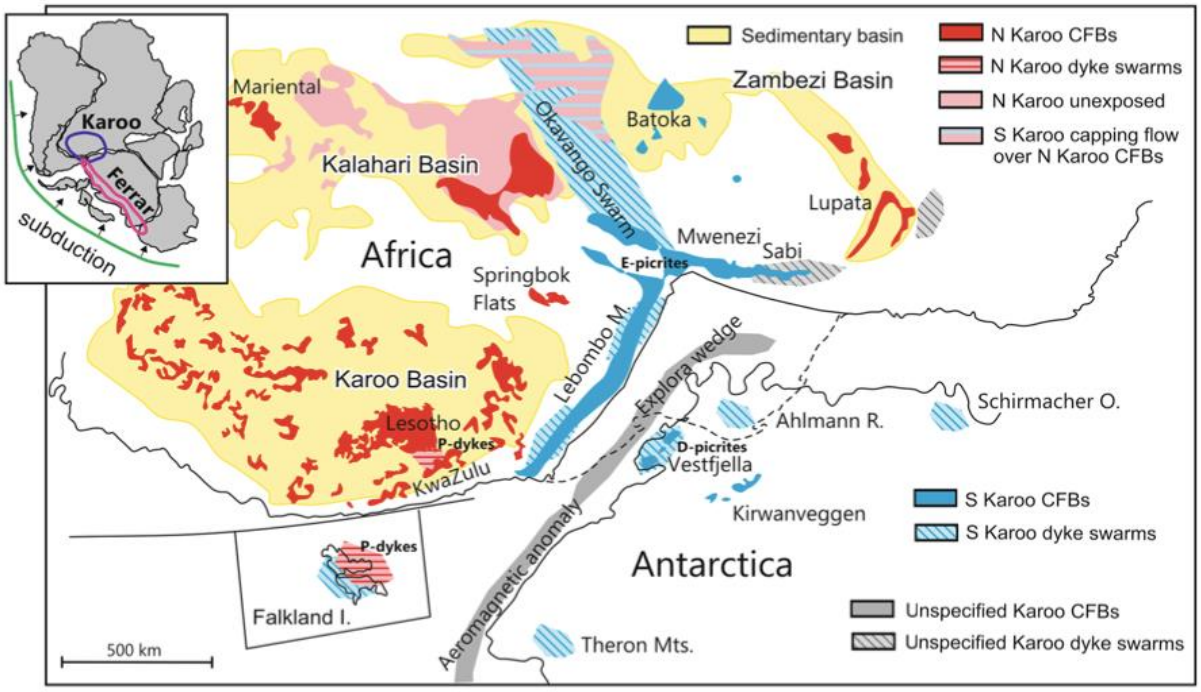

Figure 2: Map showing the Karoo Large Igneous Province (KLIP) in red and the famed Karoo Triple Junction in blue. The map depicts the prevalent tectonic regime at the time. The insert inadvertently places an emphasis on understanding how the geochemistry of the KLIP fits into the narrative of the break-up of southern Gondwana. Southern Karoo CFBs are depleted in Nb relative to Northern Karoo CFBs. The spatially limited suite basaltic suite (Drakensberg Group) is inferred form the continuous red mass labelled "Lesotho". Taken from Luttinen (2018).

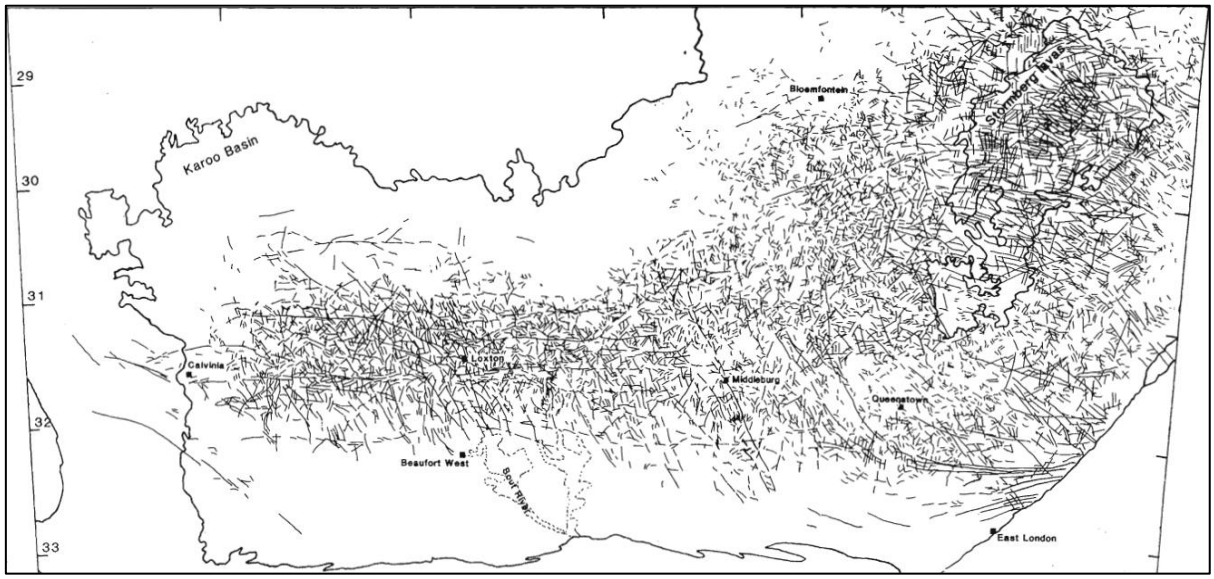

Figure 1: Seemingly random distribution of dolerite dykes in the Main Karoo basin. The assumption is made that all of these structures are Karoo dykes (i.e. dolerite and c. 180 Ma in age) *(Chevallier & Woodford, 1999)*.

The KLIP presents a chemical problem to be solved as well. Luttinen (2018) assessed spatial variation in the KLIP across much of southern Africa and presented good evidence for bilateral asymmetry in the KLIP. However, the core idea behind Luttinen's study involves the grouping of all igneous material in the Karoo basin under one banner as part of the KLIP's high-Nb province (Luttinen, 2018). A potential problem with this statement is that it fails to consider the fact that the Karoo basin covers two thirds of South Africa's total surface area (Selden & Nudds, 2012). A caveat to this potential problem is that Luttinen considered Jurassic-aged igneous material from across much of southern Africa, and not just the Karoo basin. The intrusions are connected by plumbing, but intrusion and cooling happened in isolation. That said however, the homogeneity in major element chemistry is obvious within the Karoo data used in this study (Fig. 3a) and relative to the Deccan and Siberian LIPs (Fig. 3b).

Therefore, this study has several objectives in mind. An assessment of trace elemental variation in the intrusive component of the KLIP will be conducted and, ideally, a viable emplacement mechanism that could have facilitated the intrusion of the KLIP will be proposed. It is hoped that groupings in the data are discrete and consistent throughout the geochemical analysis with strong geographic correlations. Key trace elements need to be identified in a statistically non-biased manner so that a representable analysis can be carried out.

Principal component analysis (PCA) will be used to identify clusters in the data, avoiding the systemic bias a trained geologist may impart to the data as it is quite easy to plug geochemical data into any classification diagram and accept the output. It is felt that a PCA is particularly well suited to identifying possible petrological processes driving variation in geochemical datasets. If clustering is observed in a PCA then it means that the data that are being assessed is somehow linked systematically and, because geologists understand igneous processes via systems, petrologically. If clustering is synonymous with sampling locations (i.e. geographic correlations) then the magmatism in the Karoo basin is far more diverse than previously thought.

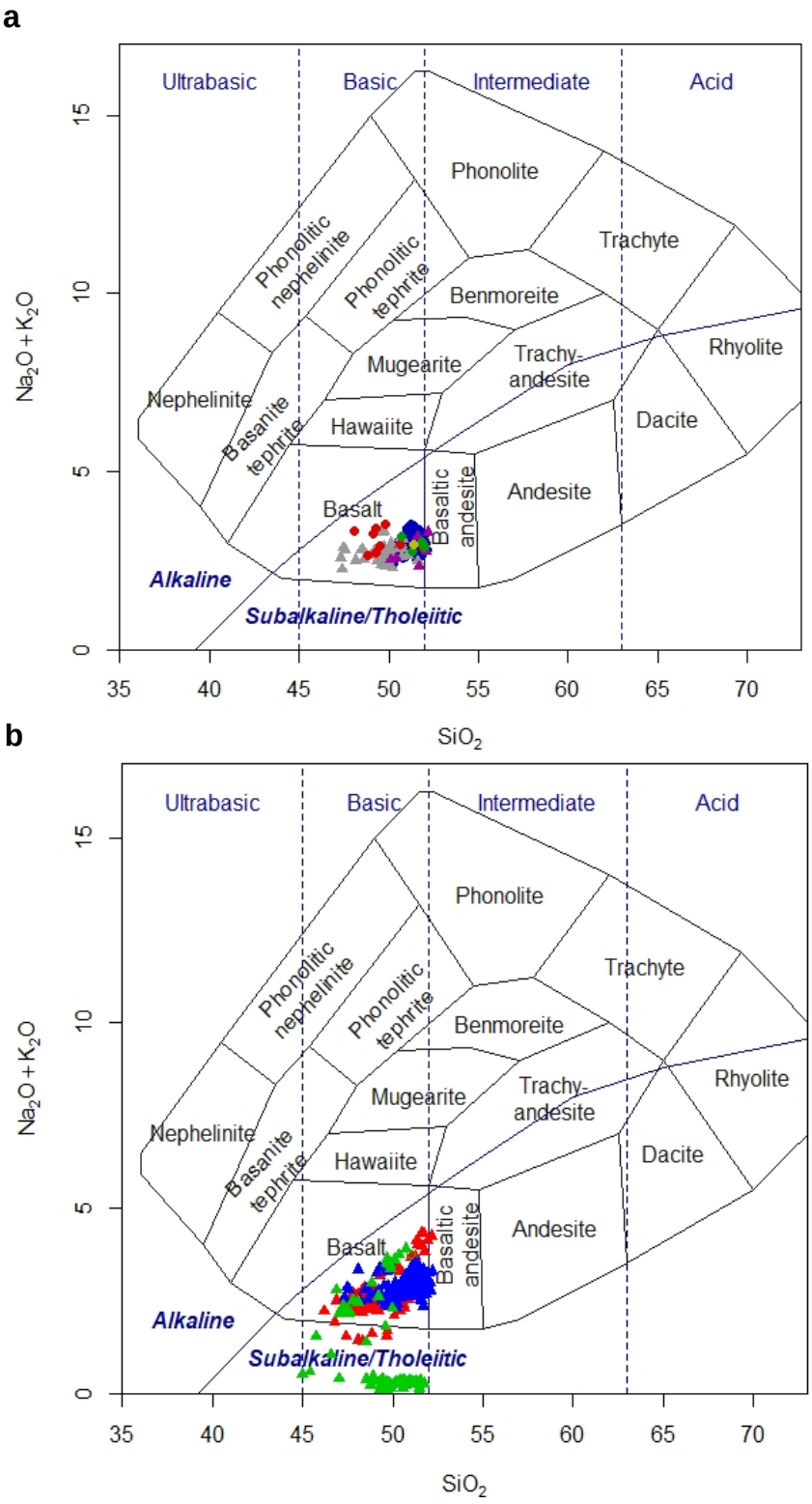

Figure 3: The top diagram (3a) shows the Karoo data in the TAS system of Cox et al. (1979). Triangles denote extrusive data and circles denote intrusive data. Grey triangles are Lesotho basalt Group 1 and purple triangles are Lesotho basalt Group 2. Intrusive data comprises data from several locations; Karoo Central Area (**KCA; yellow**), Golden Valley Sill complex (**GVS; blue**), KWV Sill (**KWV; red**) and Underberg Dyke Swarm (**UDS; green**). Figure 3b (bottom) shows the Karoo data (blue) relative to data from the Siberian (red) and Deccan (green) flood basalt provinces.

PCAs are best used as an exploratory technique prior to processing multivariate data. PCAs are also useful in addressing the problem with multi-dimensionality. This operation takes uncorrelated but known variables, converts them into correlated unknown variables, and presents the results as principal components, thereby decreasing the number of dimensions in which to view the data. The first component is responsible for the most amount of variation in the dataset, and following components are computed hierarchically. The variation imparted by the variables is presented as vectors in *n*-dimensional space as would be defined by *n* components (ideally $n \geq 2$). The power of a PCA lies in that the vectors and components can be used to infer a latent system that could be responsible for the observed variation. Obviously, if any alterations are made to the data then the PCA would have to be run again.

This study aims to place the geochemistry of the Karoo dolerites within a larger geodynamic context without preconceived notions about what should or should not be encountered. Statistical analysis of trace element chemistry will allow for a more sophisticated evaluation of the data, looking for associations/dissociations between spatial and geochemical trends in the data. Although the Drakensberg lavas are secondary to this study, they will be included in the analysis and considered coeval with and related to the dolerites, as any (or none) relationships found will offer valuable insight.

Background

The Karoo Supergroup

The Karoo basin plays host to the Karoo Supergroup, a c. 300-180 Ma sedimentary succession capped by the remnants of the Karoo Flood Basalts (Fig. 4 and 5). The Karoo Supergroup comprises four sedimentary sequences and, as mentioned, one volcanic sequence. The Dwyka Group acts as the floor of the succession, overlain by the Ecca, Beaufort and Stormberg Group (Johnson, et al., 1997) s. These sediments record major climate change during Permian-Jurassic times; indeed, a large component of the understanding of southern Africa's geodynamics and paleoclimate is based on the Karoo Supergroup (Catuneanu, et al., 2005).

The Dwyka Group is characterized by widespread diamictite, implying a glacial origin. Northern glaciation has been associated with glacial retreat, in comparison to southern glaciation which had an alpine (i.e. high lying mountainous terrain) control owing to the Cape Fold Belt (Johnson, et al., 1997). Sedimentation does seem to have had a tectonic control with continental facies preserved in northern deposits in contrast to southern deposits which demonstrate marine facies (Catuneanu, et al., 2005). The post-Dwyka paleoclimate warmed, and the Permian Ecca and Late Permian Beaufort groups.

Deltaic, fluvial, lacustrine and marine environments dominated the Karoo basin during Ecca Group times. Ecca Group outcrops are characterized as dark-coloured shales and interspersed siltstones and sandstones (Johnson, et al., 1997; Catuneanu, et al., 2005). Northern deposits are associated with lacustrine environments whereas southern deposits are associated with marine environments (Catuneanu, et al., 2005). Tuffs preserved in the Ecca Group are of a western Antarctican origin, with geochronology dating them at 265-250 Ma (McKay, et al., 2015).

Late Carboniferous to Early Jurassic times in the Karoo were characterized by depositional environments ranging from fluvial to overbank fluvial conditions, facilitating the deposition of the Beaufort Group. Northern uplift allowed for the widespread draining into an epeiric sea, and the Beaufort Group outcrops as mudrocks, sandstones and conglomerates in areas which were dominated by fluvial activity (Johnson, et al., 1996; Johnson, et al., 1997; Catuneanu, et al., 2005). Some tuffaceous material may be found in the Beaufort Group, which Catuneanu et al. (2005)

attributed to an andesitic volcano in western Antarctica or on the east coast of South America.

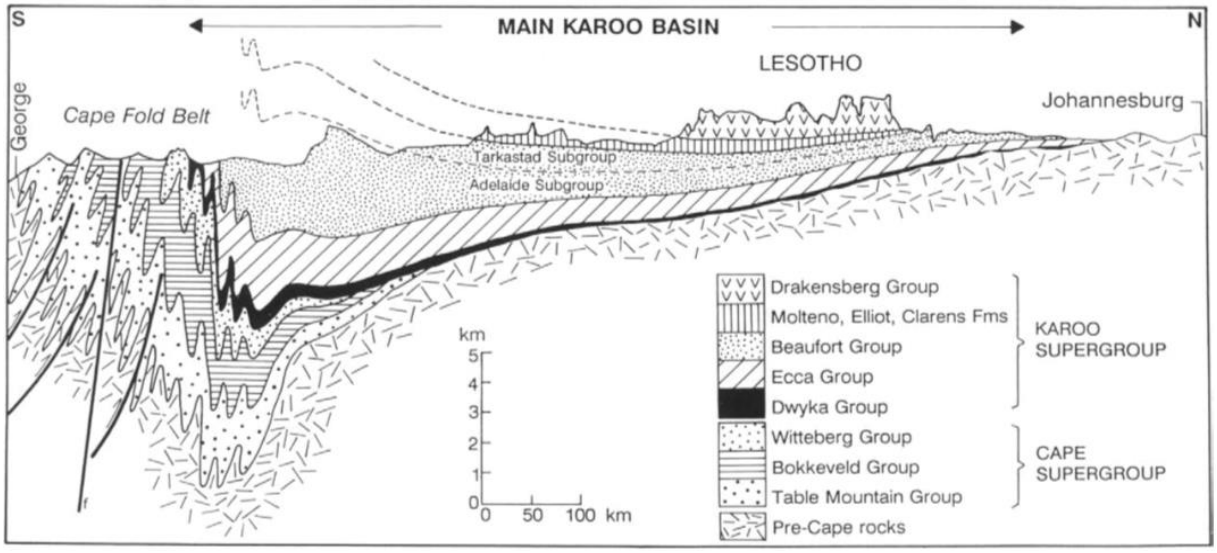

Figure 5: A cross section of the Karoo basin. Pre-Cape rocks refers to the basement rocks of the Namaqua-Natal Metamorphic Province. Taken from Johnson et al., (1997). Main Karoo basin refers to the Karoo basin as there are other Karoo-aged basins in southern Africa (*(Catuneanu, et al., 2005)*.

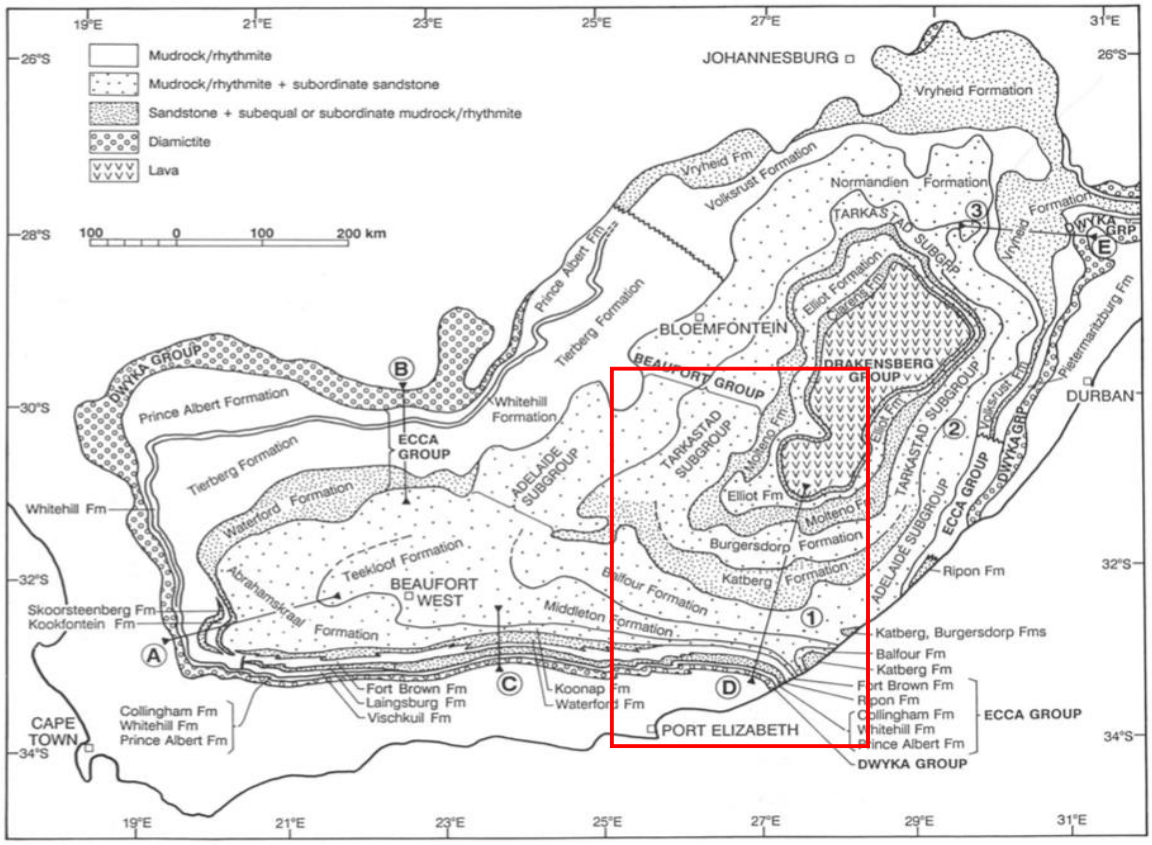

Figure 4: Map showing the outcrops of the Karoo Supergroup. Taken from Johnson et al. (1997). The red rectangle shows an approximation where Figure 6 can be found on this map.

The Triassic to Early Jurassic stratigraphical units of the Stormberg Group are the Molteno, Elliot, and Clarens Formations, respectively. Increasing aridity was also accompanied by continued marine regression which eventually allowed for the aeolian features of the Clarens Formation Group to form. Minor lava flows have been preserved in the upper Clarens Formation as well, signalling the end of Karoo Supergroup sedimentation and the start of the Karoo Flood Basalts (Johnson, et al., 1996; Johnson, et al., 1997; Catuneanu, et al., 2005).

The extrusion of the Karoo Flood Basalts started c. 183 Ma, although Karoo volcanism probably started earlier than that considering the tuffaceous material in the Clarens and Elliot Formations (Johnson, et al., 1997). The Sterkspruit Complex, Lesotho (Fig. 6), holds convincing evidence (pillow basalts, playa lakes and lava pod complexes; all *in-situ*) of a phreatomagmatic event, after which effusive activity resulted in tholeiitic pahoehoe type flows (McClintock, et al., 2002). Flow units lower down in the Drakensberg Group have preserved amygdaloidal textures (Johnson, et al., 1997).

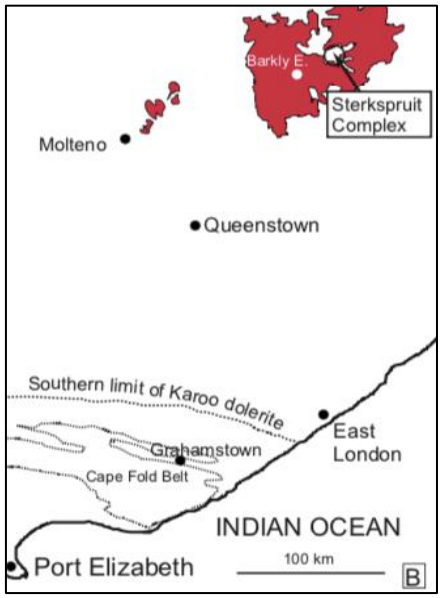

Figure 6: Drakensberg Group flood basalts are shown in red. The location of the Sterkspruit Complex is indicated. Modified from McClintock et al. (2002).

Moulin et al. (2011) used K-Ar dating to identify two discrete periods of effusive activity within the Karoo Flood Basalts, also finding that older flows are thicker than younger flows. The Drakensberg Group lava flows were extruded c. 3-5 m.y. after the first volcanoclastic material was deposited in the Elliot Formation (Moulin, et al., 2011). Smith et al. (1993) recorded little signs of weathering in between various flow units, concluding that flows were extruded over a short period of time. Smith et al. (1993) have been corroborated by $^{40}Ar/^{39}Ar$ dating from Jourdan et al. (2007a) and Moulin et al. (2017). Moulin et al. (2017) used palaeomagnetic data as well as K-Ar dating.

Jourdan et al. (2007a) and Moulin et al. (2017) places the effusive activity in a period less than 800 kyr. Moulin et al. (2017) estimates that this number might be closer to 250 kyr with the main phase of activity occurring between 182.8 ± 2.6 and 180.1 ± 1.4 Ma. This main phase of activity refers to much of the intrusive and extrusive magmatism observed in the Karoo basin (Moulin, et al., 2017). New data from Greber

et al. (2020) places most of the intrusive material at c. 183 Ma using $^{40}Ar/^{39}Ar$ and provides evidence that Karoo volcanism was active at c. 176 Ma using U-Pb. (Greber, et al., 2020).

The Karoo basin

The most popular model for the Karoo basin (Fig. 7) differentiates the basin into the typical proximal foredeep, central fore-bulge and distal back-bulge flexural provinces expected from a retro-arc foreland basin (Catuneanu, 2004; Bumby & Guiraud, 2005; Johnson, et al., 2006; Götz, et al., 2018). In this model, eastward-trending subduction occurs to the west of the Cape Fold Belt, the continued deformation of the Cape Fold Belt loads the underlying crust, and the crust bends accordingly. The foredeep would have been an epeiric sea and the back-bulge flexural provinces would have been in relief relative to the foredeep. The sedimentary record of the Karoo basin corroborates well with this model, hence its popularity.

In contrast, Tankard et al. (2009) interpret the Karoo basin as a product of initial

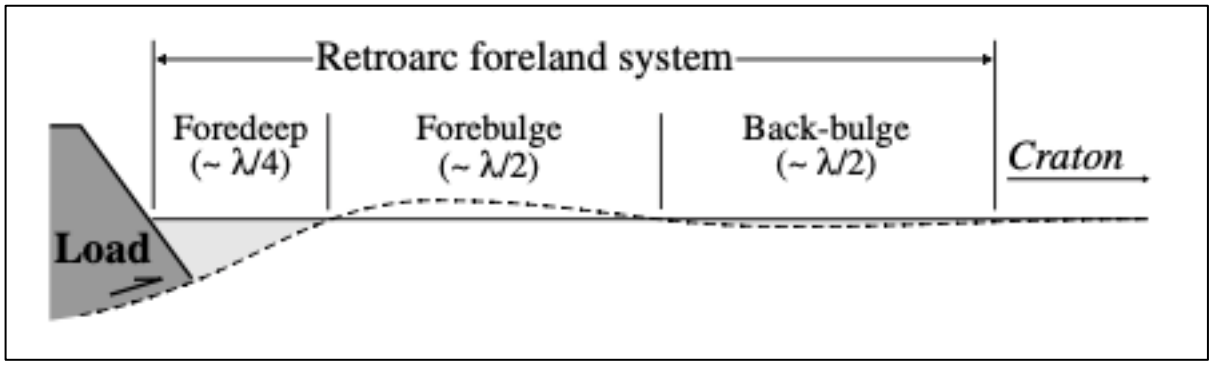

Figure 7: Diagram showing the flexural mechanics at work in a conventional retro-arc foreland basin. The symbol λ is used to show flexural wavelength. Flexing is attributed towards orogenic loading. Modified from Catuneanu (2004).

uplift and prolonged subsidence (Fig. 8) and structures can be inferred from the variation in densities shown (Feininger & Seguin, 1983). It is pointed out that the retro-arc model requires a subduction zone adjacent to the foredeep but there is no evidence of subduction or a volcanic arc in the Cape Fold Belt itself. Although the Cape Fold Belt probably did load the basement rocks of the Namaqua-Natal Metamorphic Province (NNMP), Tankard et al. (2009) argue that subsidence is not attributed to flexural mechanics. Rather, Tankard et al. (2009) attribute subsidence to induced mantle flow from the subduction along the southern margin of Gondwana. Vertical movement of crustal blocks bound by crustal-wide discontinuities (e.g. the Doringberg

Fault, Tugela Shear Zone, Lilani-Matigulu lineament, etc.) is used to describe the formations of the respective depo-centres of the Karoo Supergroup.

Figure 9 shows a model which places the Karoo basin behind the Cape Fold

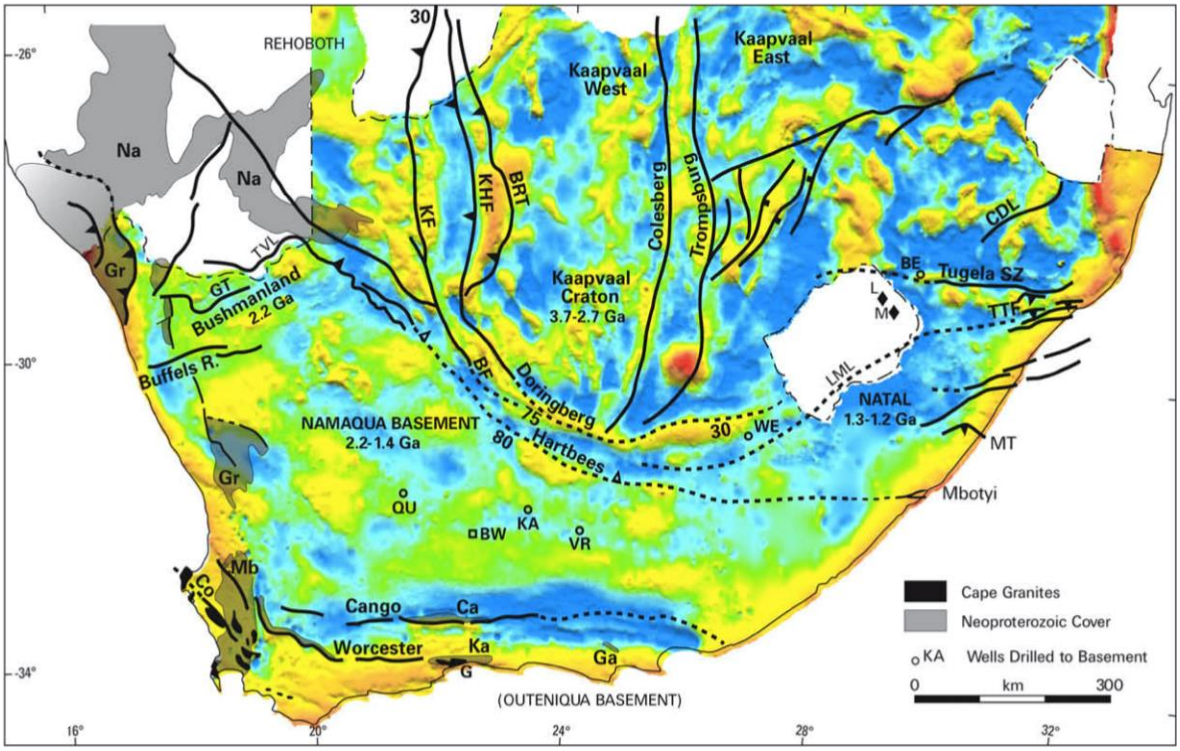

Figure 8: Bouguer gravity anomalies showing the crustal structure of South Africa underlying the Main Karoo basin. BF: Brakbos fault; BRT: Blackridge thrust; CDL: Commondale lineament; Ca: Cango Caves Group; Co: Colenso fault; G: George; Ga: Gamtoos Group; Gr: Gariep Group; GT: Groothoek thrust; Ka: Kaaimens Group; KF: Kalahari fault; KHF: Kheis fault; L: Letseng-la-Tarae kimberlite; LML: Lilani-Matigulu lineament; M: Matsoku kimberlite; Mb: Malmesbury Group; MT: Melville thrust; Na: Nama Group; TTF: Tugela thrust front. Modified from Tankard et al. (2009).

Belt as part of a Jura-type fold belt (Lindeque, et al., 2011). The model assumes that the Cape Fold Belt is deformed in upper crustal thin skinned folds due to either arc accretion, a continent-continent collision or merely some kind of southern suturing. This neatly accounts for the lack of subduction in the Cape Fold Belt and places the deformation of it within an acceptable geodynamic narrative (Lindeque, et al., 2011). However, Lindeque et al. (2011) does not explain the formation of the Karoo basin itself.

The Karoo ring-dyke complexes

Referring to the intrusive component of the Drakensberg Group as “ring-dyke complexes” is a slight misnomer. The formation of ring-dyke complexes is generally associated with calderas (Andersson, et al., 2013), and the Karoo basin is obviously not a caldera. However, the morphology of these arcuate structures adheres to the physical characteristics of ring dykes as described by Macdonald (1989). Figure 10 illustrates the inter-sill relationships seen in the Golden Valley Sill Complex. One ring-dyke complex can often have several sills emplaced at various stratigraphic heights (Thomson, 2004). Thomson (2004) interprets this as evidence for magma travel along regional conduits.

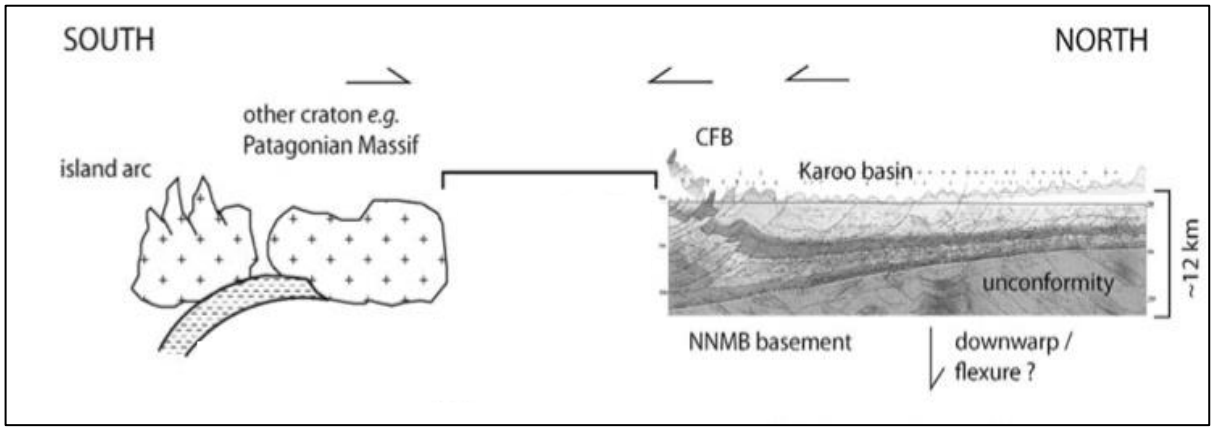

Figure 10 (top): Thin-skinned Jura-type fold belt model for the Cape Fold Belt. Vertical movement is recognized but attributed towards flexural mechanics in contrast to subsidence as in Tankard et al. (2009). . NNMP refers to the Namaqua-Natal Metamorphic Belt. Modified from Lindeque et al. (2011).

Figure 10 (right): A map of the Golden Valley Sill Complex. Here the general structural configuration of the ring-dyke complexes may be observed well. GVS, Golden Valley Sill; GS, Glen Sill; HS, Harmony Sill; MS, Morning Sun Sill; L1, L1 sill; GVD, Golden Valley Dyke *(Neumann, et al., 2011)*.

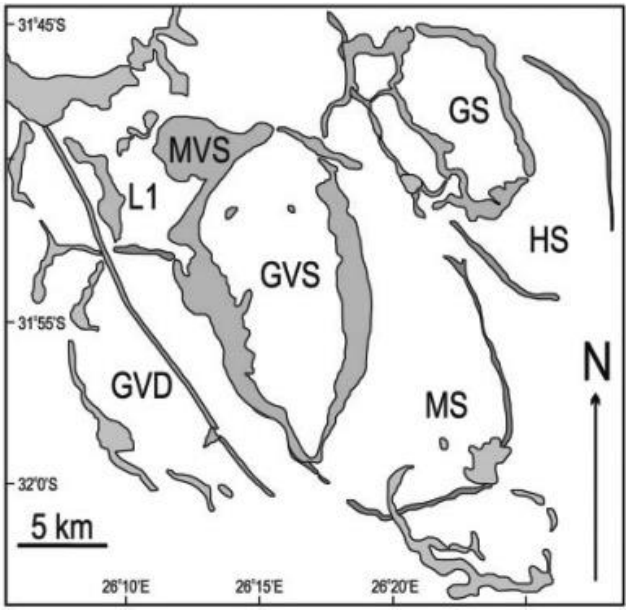

Chevallier & Woodford (1999) defined the structural geometry of the ring-dyke complexes as comprising three components: i) a feeder dyke feeds into inclined arcuate sheets forming an ii) outer sill that eventually feeds into an iii) inner sill through

gravity (i.e. the outer sill falls back in on itself to form the inner sill) (Fig. 11). Malthe-Sørensson (2004) looked at this model and suggested that instead of the inner sill being gravity fed from the outer sill, the inner sill (1) propagates into the outer sill (2). A central feeder dyke drives the emplacement of the ring-dyke complex from below (Fig. 12). Coetzee & Kirsters (2017) turned Chevallier & Woodford's model inside out, suggesting that the propagation of the inner sill controls the formation and orientation of dykes. This model is comparable to the "cracked roof" model used to describe similar intrusions in Antarctica (Muirhead, et al., 2014).

Some strides have been made in identifying the physical mechanism through which these ring-dyke complexes are emplaced in the host rock. Polteau et al. (2008) suggested that there is a relationship between the deformation of the overlying strata and low viscosity fluid filled hydraulic fractures. Since both components would have a control on the leading edge of the sill, the sill would propagate accordingly (Polteau, et al., 2008). In comparison to hydraulic fracturing of the host rock, Mathieu et al. (2008) postulate that the shear failure of the host rock allows for the propagation and emplacement of the ring-dyke complexes. Galerne et al. (2011) concur with the shear failure model concluding that shear failure of the host rock seems to provide a better account for the physical shape of these complexes than the hydraulic fracturing model.

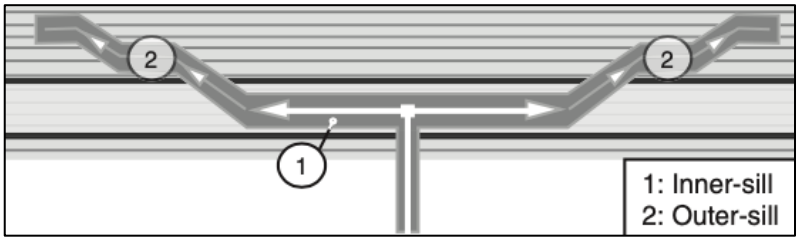

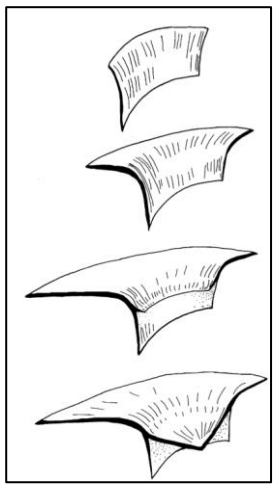

Figure 12: (right) Three component system responsible for the formation of ring-dyke complexes according to Chevalier and Woodford (1999).

Figure 12: (top) Model of magma travel during ring-dyke construction and emplacement. The propagation of the inner sill controls the formation and orientation of the dykes *(Malthe-Sørrenson, et al., 2004)*

Broad geochemical overview Karoo dolerite

There are two Nb-provinces in the Jurassic-aged igneous material across southern Africa (Fig. 1). The southern Karoo CFBs are Nb-depleted and the northern Karoo CFBs are Nb-enriched relative to one another (Luttinen, 2018). According to Luttinen (2018), the Nb-rich province could be indicative of a plume component whereas the Nb-poor province could be a result of crustal contamination.

Neumann et al. (2011) studied the evolutionary history of dolerites from the Golden Valley Sill Complex with an emphasis placed on the melts from which these dolerites are derived. The proposed primary melt origin is metasomatized lithospheric mantle (Neumann, et al., 2011). One of the outcomes of Neumann et al. (2011) is a suggestion that the Karoo volcanics were either derived from spatially different (but geochemically similar) SCLM regions (Neumann, et al., 2011). Although Neumann et al. (2011) provides a well-substantiated model for the evolutionary history of the Golden Valley Sill Complex in Figure 13, their model inadvertently relies on magma entering the Karoo basin from multiple entry points but does not locate these entry points.

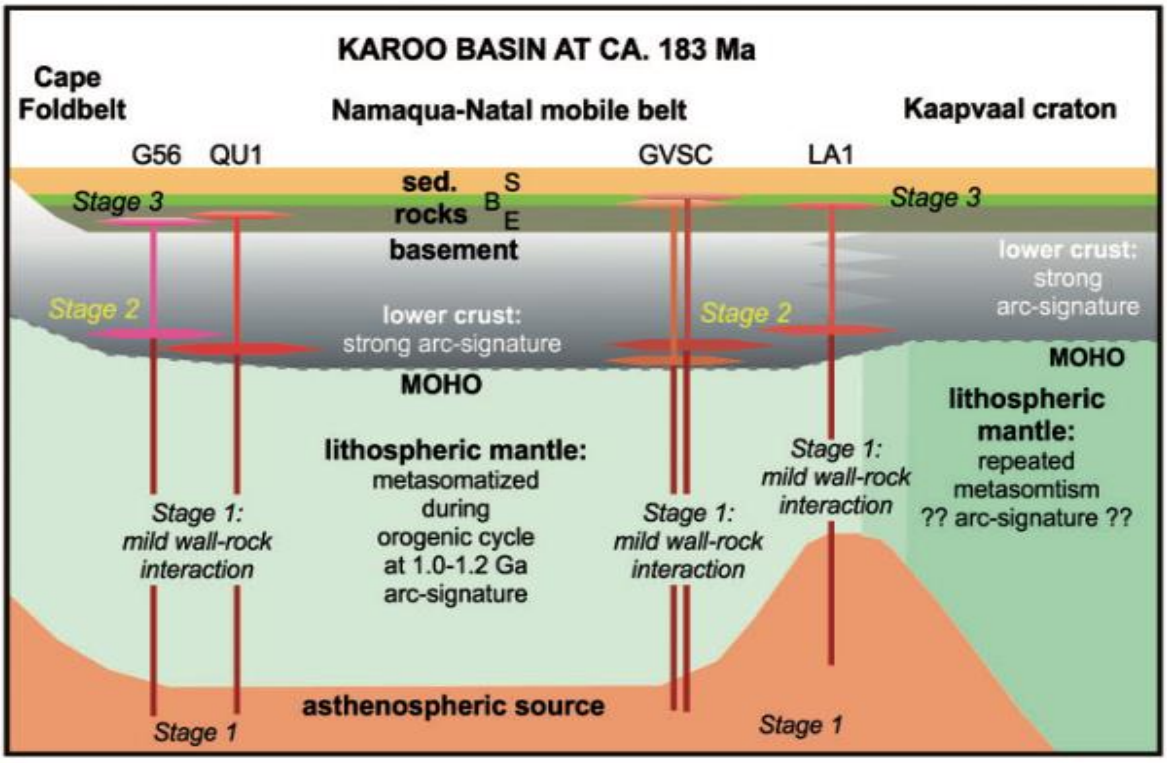

Figure 13: Neumann et al.'s (2011) model for the petrogenisis of the dolerites in the Karoo basin.

The Karoo mantle plume

Plume theory is mainly drawn from the recognition of surface structures and their corroboration with mathematical models. Structurally, a mantle plume includes a large plume head (c. 1000 km diameter) and a tail that narrows with depth. A c. 1000 m uplift of the land surface precedes the eruption of flood basalts. Mantle plumes generates high abundances of picrictic lavas with progressively lower abundances found with increasing distance from the plume head (Campbell, 2006). Radial dyke swarms are closely associated with mantle plumes intersecting continental crust (Eriksson, et al., 2002). Campbell (2006) concludes by saying that although there are

some clear-cut cases of plume volcanism (Hawaii is a good example), each occurrence must be considered unique unto its own.

The Nb-depleted southern Karoo lavas (Fig. 1) have a structure that bears a striking resemblance to a triple junction. This structure is ingeniously referred to as the Karoo Triple Junction (Jourdan, et al., 2006) and is inferred from the orientations of the Okavango Dyke Swarm, Save-Limpopo Dyke Swarm (depicted as the Mwenezi-Sabi limb on Fig. 1), and the Lebombo Monocline (Hastie, et al., 2014). The Karoo Triple Junction has become synonymous with plume activity because of the surficial structure of the triple junction, triple junctions in general being associated with continental break-up, and mantle plumes sometimes being the cause of continental break-ups (Beniest, et al., 2017).

The KLIP is attributed to plume activity for a variety of reasons: the presence of dyke swarms, the sheer volume of magma thought to be present in the KLIP (c. $3x10^6$ km^2), and flood basalt provinces commonly being attributed to plume activity (as discussed in Hastie et al. (2014) and references therein). The KLIP is also associated with the c. 180 Ma disassembly of southern Gondwana, which has been ascribed to plume activity as well (Elliot & Fleming, 2000).

Other work done with principal component analysis

The appeal of a principal component analysis (PCA) partly lies in its ability to process large amounts of multivariate data quickly (Everitt & Hothorn, 2011), partly in providing sources of variation in the data, and partly in producing inferences. If a PCA is performed on trace elemental data then latent systematic relationships between multivariate data can be inferred (however if something interesting is observed then it will have to be corroborated with more formal geochemistry). Therefore, processing igneous data with a PCA can be thought of as an attempt to associate the behaviour of trace elements with an igneous system. This makes a PCA particularly well suited to geologists trying to understand geochemical problems as it can be applied to any multivariate dataset drawn from any tectonic setting.

Good examples of this can be found as Thy and Esbensen (1993) and Ueki and Iwamori (2017). The Troodos complex in Cyprus has been described as a thin layer of ultramafic oceanic crust in a back-arc basin (Thy & Esbensen, 1993). Using a PCA, Thy and Esbensen (1993) assessed a multivariate dataset with more than 500 samples and concluded with saying that only the upper gabbros, the dike complex, and the

lower lava sequence are products of seafloor spreading. Ueki and Iwamori (2017) used PCAs to find that the chemistry of the Sengan volcanic cluster, northeast Japan, is largely controlled by magma mixing and other crustal processes.

A PCA is highly sensitive to the relative variation in the data that is being processed. Storrie-Lombardi and Fisk (2004) could differentiate biotic and abiotic alteration of seafloor basalts using a PCA and a hierarchical cluster analysis algorithm. Numerical assessments had a high correlation with visual assessments (Storrie-Lombardi & Fisk, 2004). The sensitivity of a PCA is enough to differentiate legally mined gold from illegally mined gold (Roberts, et al., 2016). Ideally, gold should be traced back to the mine that produced it but illegal gold can be a mixture from several mines. Roberts et al. (2016) could identify illegal gold by the variation imparted by trace elements that is not common to legal gold.

Methodology

Data description

A database of Karoo data was downloaded from GeoROC, an online geochemical data depository (Sarbas & Baerbel, 2008) queried via continental flood basalts and location; URL: http://georoc.mpch-mainz.gwdg.de/georoc/ [Accessed: 30 March 2019]). This database was then complimented by intrusive data graciously provided by Prof. Nils Lenhardt of the Geology Department at the University of Pretoria; these currently form part of an MSc project by Ngeleka (submitted 2021).

Criteria for sample selection was based on analytical error margins, SiO_2 content (i.e. rock type) and the sampling location. The data was therefore filtered according to the reported total wt% measured, using an error margin of ± 1.50 wt-% from 100.00 wt-%, and filtered to only include basalts by using a SiO_2 range of 44.75% to 52.25%. Any sample that exceeded this analytical error, was not a basalt, and was not sampled in the Karoo basin, was excluded from the dataset. The initial dataset of 179 samples evolved into the dataset used in this study and comprised 139 rocks: 49 basalts and 90 dolerites. The same set of filters were applied to the data from the Deccan and Siberian basaltic provinces in Figure 3b.

Five sampling locations were identified; one for the basalts and four for the dolerites (Fig. 14). The basalts were sampled in Lesotho by Marsh et al. (1997): 12 from the Springbok Flats Formation, 17 from the Barkly East Formation, and 20 from the Lesotho Formation. Washington State University oversaw whole-rock chemical analysis as well as palaeomagnetic studies. Major and trace elements were determined by wave-length dispersive XRF on 2:1 fusion dilution beads as per Hooper et al. (1993). Rare earth elements (REEs), U, Pb, Th, Hf, and Ta were determined by ICP-MS, also at Washington State University (Marsh, et al., 1997). These basalts were grouped into one sampling population for this study.

The dolerites were sampled in a roughly east-west trend across the Karoo basin. The two smallest sampling populations are those of the Karoo Central Area, near Sutherland (one sample; abb. KCA), and Underberg (five samples; abb. UDS). The KCA data were derived from Ware et al. (2018). Major element analysis was done by XRF on fused discs. ICP-MS was used for analysing trace elements on samples dissolved using a lithium metaborate/tetraborate fusion. All analyses were done at Genalysis Laboratory Services Pty Ltd in Perth, Australia (Ware, et al., 2018). Similarly,

the UDS data were drawn from Riley et al. (2006). The Department of Geology, University of Keel, oversaw whole-rock analysis using standard XRF as governed by Floyd (1985). Trace element analysis was done via ICP-MS at the University of Durham with analytical methods, precision, and detection limits according to Ottley et al. (2003) (Riley, et al., 2006).

The bulk of the intrusive data comprised 74 samples from the Golden Valley Sill complex (abb. GVS) and 10 from the KWV sill near Willowvale in the Eastern Cape

Figure 14: Map showing the sampling locations of data used in this study. Sampling of intrusive material occurred in, and moving from left to right, 1) the Karoo Central area (KCA), 2) Golden Valley Sill complex (GVS), 4) KWV sill, and 3) Underberg Dyke Swarm (UDS). Extrusive material is divided into a 5) southern and 6) northern group of basalts (LB1 and LB2, respectively) based on relative K and Na contents *(Google Earth, 2020)*.

(abb. KWV). The GVS data is taken from Neumann et al. (2011). Major and trace element chemistry were determined by inductively coupled plasma atomic emission spectrometry (ICP-AES) and ICP-MS at the University of London, Royal Holloway (Galerne, et al., 2008).

The data for the KWV sill is drawn from Ngeleka (submitted 2021) Whole-rock analysis using XRF was done at the Stoneman Analytical Laboratory, University of Pretoria. Trace elements were analysed at AEON EarthLAB of the University of Cape Town using a Thermo Fisher Xseries II for ICP-MS. The KWV data reported Fe as Fe_2O_3 whereas the GeoROC data reported iron as FeOt; a conversion factor of 0.8899 was applied to address the disparity.

Data processing

Major element chemistry was briefly examined using standard geochemical diagrams. The TAS diagram (Fig. 3) from Cox et al. (1979) was selected over that of Le Bas et al. (1986) and Middlemost (1994) due to the 5% increments in SiO_2 content. Only trace elements that were mutual to all studies were used so any conclusion drawn from these trace elements will need to be re-evaluated in the future as more trace elements become available for study. The trace elements common to all sampling locations were Cr, Co, Ni, Rb, Sr, Y, Zr, Nb, and Ba. Although La, Ce, and Nd were mutual to all studies, not all basalts had values recorded for these elements. Trace elements that were mutual to all studies save one (KCA) are V, Cu, and Zn. This totals to 15 trace elements that can be used to generate representative results in this study. Of these elements, two are high-field strength elements (HFSE; Nb and Zr), three are large ion lithophile elements (LIL; Ba, Sr, and Rb), four are rare earth elements (REE; Ce, La, Nd, and Y), and six are transition metals (Co, Cr, Cu, Ni, V, and Zn).

Principal component analyses were carried out to diagnose which elements are active participants in driving variation and which are passive bystanders. However, a principal component analysis can only compute components using as many variables as there are data entries, or in the case of this study, samples. For example, the KCA data had one sample, so any principle component analysis where KCA data is present in could only be computed using one variable, which would not produce a meaningful result.

The inclusion of the KCA data, then, had more to do with observing its behaviour as GVS, KWV and LB1 data were being compared to one another. UDS and LB2 data received comparable treatment for similar reasons. UDS data, at five samples, had no values recorded for V and LB2 data had only seven samples. Were the LB2 data included then any PCA would only have yielded seven components instead of 10 in the case of its exclusion. It was felt that the representability of the PCAs would be furthered if as many feasible variables as was possible could be included in the calculation.

Arguably the most attractive feature of a PCA was its ability to process large volumes of data quickly and efficiently, showing clusters and outliers (provided there are clusters and outliers in the data) as well as expressing important variables as vectors. This allowed for easy interpretation of which variables had more influence on which component(s). Possible latent magmatic processes could be inferred from this

since igneous rock could be considered an amalgamation of igneous processes frozen in time. However, these inferences are just that: inferences. A PCA is an exploration of multivariate data and should thus not be used to quantify multivariate data (Everitt & Hothorn, 2011). In other words, a PCA can be used to explore how the data is linked systematically, but cannot be used to make definitive statements about the data.

A geochemical investigation was done using the trace elements identified by the PCA. This ensured that these elements were the focal point from which to start the broader investigation and not assumed knowledge about the KLIP. It is hoped that a clear look at magmatic evolution of the KLIP can be garnered by simply adhering to that what the data can provide. Graphical representations and statistical analysis of the data was done using GCDkit, a system for the handling and recalculation of whole-rock analyses for igneous rocks. GCDkit is written in R, which is a language and environment for statistical computing and graphics (Janousek, et al., 2006). The results tables for the PCA were generated using R.

Results

Major element chemistry

Major element chemistry is a poor indicator of progressive magmatic evolution for a variety of reasons (but works well for classification). Major elements usually account for most (>99%) of the constituents in an igneous system but, relative to trace elements, show very little variation. This is compounded by trace elements being far more susceptible to changes in the physical environment of the magma; the variation imparted by trace elements can easily be an order of a magnitude (or several) higher than that of major elements. Trace elements can also be used to partially discriminate igneous processes from one another, e.g. differentiating fractional crystallisation from partial melting (White, 1999).

Major element data from the Karoo volcanics falls in the sub-alkaline or tholeiitic and basaltic fields of Figure 15. Since the demarcation between these two rock types is more of a spectrum than a discrete chemical boundary (White, 1999), the igneous data from the Karoo basin can be classified as being tholeiitic basalt. Interestingly, the dataset is remarkably homogenous within the relatively small basalt field and relative to the basalts of the Deccan and Siberian flood basalt provinces (Fig. 3b). The dolerites from the Golden Valley Sill (GVS) and KWV sill (KWV) are separated by about 270 km (Fig. 14). Figure 15 separates GVS and KWV data by 2-3% SiO_2 (Na_2O+K_2O behaviour is similar). The dolerites from the Underberg Dyke Swarm (UDS) trend more towards GVS data.

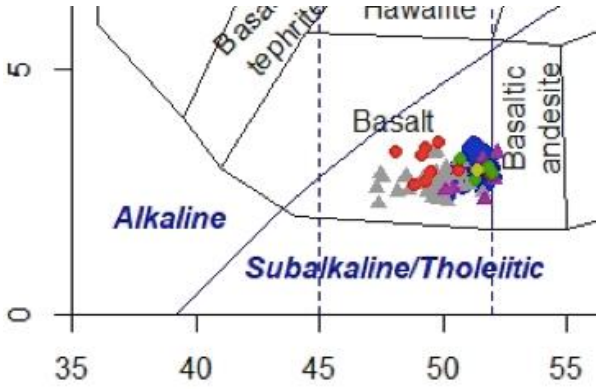

Figure 15: Close up of the spread in data from Figure 3a. Triangles denote extrusive data and circles denote intrusive data. Grey triangles are Lesotho basalt Group 1 and purple triangles are Lesotho basalt Group 2. Intrusive data comprises data from several locations; Karoo Central Area (**KCA; yellow**), Golden Valley Sill complex (**GVS; blue**), KWV Sill (**KWV; red**) and Underberg Dyke Swarm (**UDS; green**).

The 2-3% SiO_2 separation is reflected in the Lesotho data. Group 1 basalts are enriched in CaO and Na_2O and depleted in MgO and K_2O relative to Group 2 basalts (Fig. 16), hence the seemingly uniform behaviour of Na_2O+K_2O. The disparity is not reflected in TiO_2, Al_2O_3, FeOt, or P_2O_5. Group 2 is more evolved than Group 1 if one

looks at the average SiO_2 content (51.4 wt-% as opposed to 49.7 wt-%) but more primitive if MgO is considered (10.7 wt-% in comparison to 6.8 wt-%).

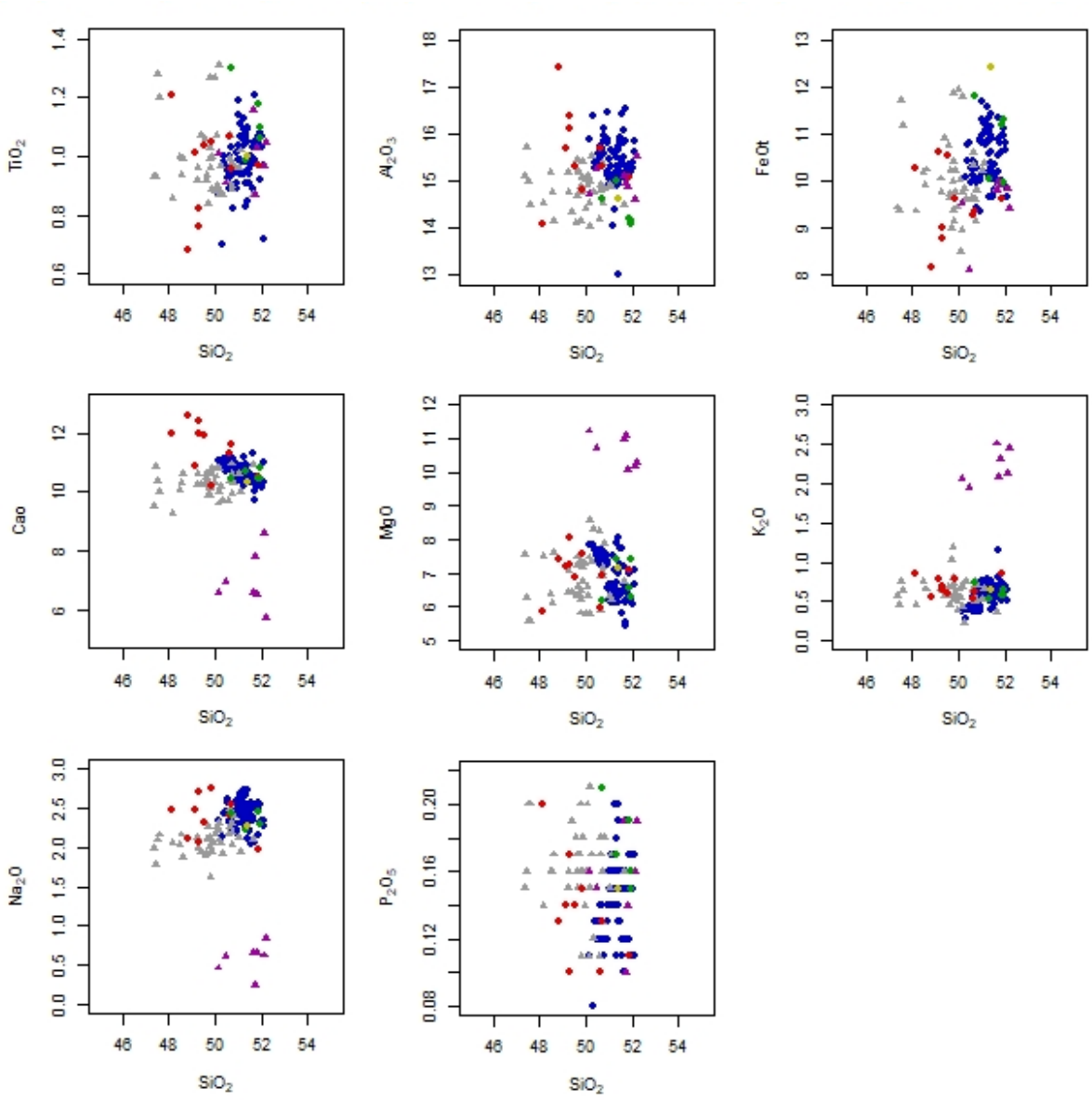

Figure 16: Harker diagrams of major element chemistry measured against an increase in SiO_2 content. Triangles denote extrusive data and circles denote intrusive data. Grey triangles are Lesotho basalt Group 1 and purple triangles are Lesotho basalt Group 2. Intrusive data comprises data from several locations; Karoo Central Area (**KCA; yellow**), Golden Valley Sill complex (**GVS; blue**), KWV Sill (**KWV; red**) and Underberg Dyke Swarm (**UDS; green**).

Although the UDS data overlaps with the other intrusive data, there is slight enrichment in TiO_2 and P_2O_5 and depletion in Al_2O_3 relative to the GVS and KWV data. Interestingly, the behaviour of Group 1 Lesotho basalts mirrors most of the behaviour of the UDS dolerites. Exceptions to this are FeO_t and TiO_2 where the UDS data mimics the behaviour of GVS data rather than Group 1 basalts (Fig. 17 allows for a closer look).

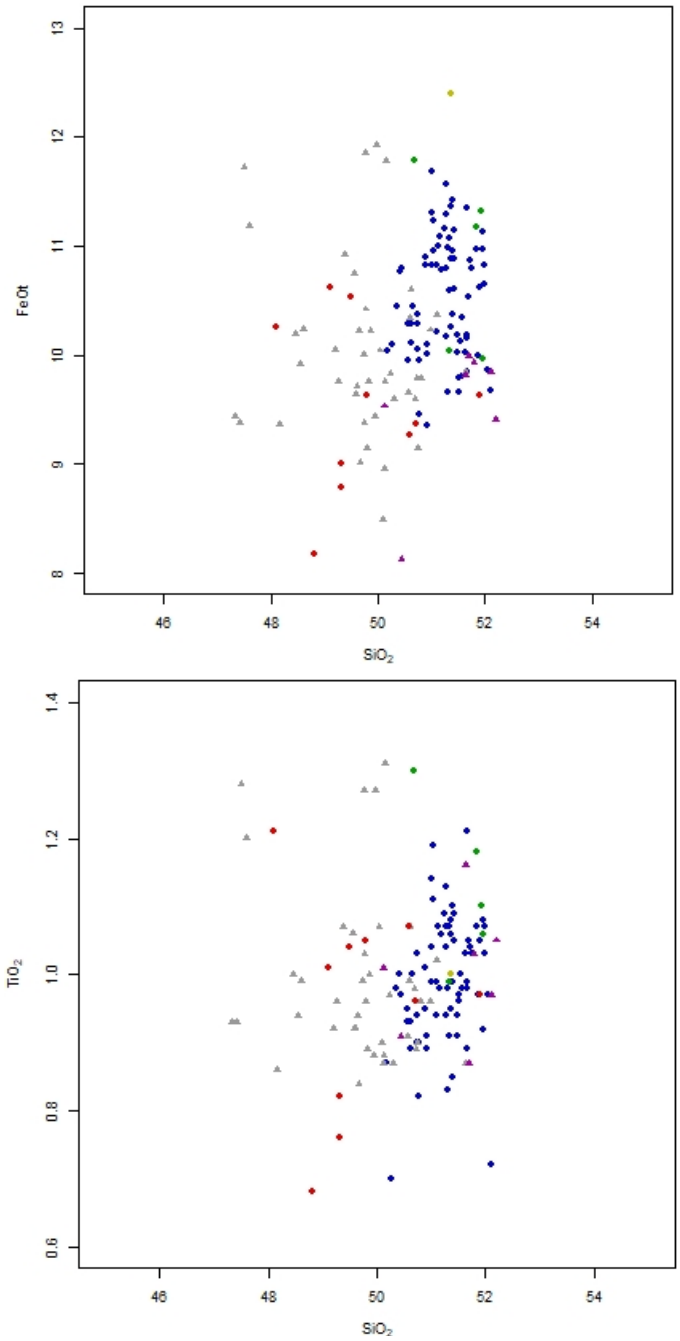

Figure 17: Binaries of FeOt and TiO_2 relative to SiO_2. The UDS data mimics the behaviour of GVS data rather than Group 1 basalts and KWV data is more conformable to LB1 basalts than to GVS data. The separation between LB1 and LB2 basalts is apparent in both binaries.

With the rather small sample sizes of the KCA and UDS datasets, this leaves the GVS and KWV datasets as the key sampling data in this study. The larger sample sizes for these two locations allow for more observable variation in the GVS and KWV data simply because there is more data to look at. The GVS data is generally slightly more evolved than the KWV data; the average SiO_2 content is higher (51.3% as opposed to 49.7%) and the average MgO content is marginally lower (6.8% as opposed to 7.0%).

There is a difference in the general behaviour between the GVS and KWV data; GVS data seems to cluster far more readily than KWV data. The largest spread in GVS data is in TiO_2, MgO, and P_2O_5 whereas the tightest clustering can be observed in CaO, K_2O and Na_2O. Variation is minimal in Al_2O_3 and FeO_t. In comparison to this, KWV data clusters only in K_2O. Increasing TiO_2 and FeO_t and decreasing Al_2O_3, CaO, and P_2O_5 in the KWV data seems to follow an increase in SiO_2. Most of the KWV data seems to show an initial increase in MgO before a decrease in MgO as the magma evolves. Variation of KWV data in Na_2O does not seem to cluster or follow a distinct trend.

Transition element chemistry

Trace elements have larger variation than major elements due to their heightened sensitivity towards igneous processes (White, 1999). Although there are only 15 trace elements with which to fabricate a representable narrative, some insightful observations can be made. Of the 15 elements, three are large ion lithophile elements (Ba, Rb, and Sr); two are high field strength elements (Nb and Zr); four are rare earth elements (Ce, La, Nd, and Y); and six are transition metals (Co, Cu, Cr, Ni, V, and Zn). Since a principal component analysis (PCA) is essentially a flashlight for multivariate data, it can be used to look at certain aspects of the data and not just the whole. The exploratory nature of a PCA means that any variation that is found must be attributed towards something (otherwise the variation would not be there to begin with). Only then can the decision be made if the variation is relevant to that which is being studied.

A PCA computes principal components out of a matrix and presents relevant variables as vectors in a space defined by the components (Everitt & Hothorn, 2011). The “importance” of any variable is inferred from the magnitude of the vector relative to the component; this is referred to as the loading of the variable. Geologists have come to interpret and understand magmatic evolution in terms of the behaviour of different groups of elements under different sets of environmental controls. Instead of basing a geochemical investigation off the results of what can be considered a bulk PCA (that is, one PCA calculating two or three components out of the whole dataset), the geochemical investigation can be fine-tuned to the different behaviours of LILs, HFSEs, and REEs.

The behaviour of compatible transition metals is usually a stronger function of the composition of the magma than that of incompatible trace elements. Transition metals, with their highly directional *d*-orbitals, also have a propensity to form covalent bonds instead of ionic bonds. This means that the solubility of these metals is controlled by the valence state of the metal in question as well as the availability of an anion with which to form a complex (White, 1999).

The two principal components shown in Figure 18a accounts for approximately 96% of the total variation in the transition metals (Co, Cu, Cr, Ni, V, and Zn; Table 1). Component 1 (c. 90% of variation) sees a weak positive loading from V, a weak negative loading from Ni, and a strong negative loading from Cr (Table 2). Component 2 (c. 6% of variation) sees a weak positive loading from Cr, moderate positive loadings from Zn and Cu, and a strong positive loading from V. Elements imparting negative loadings on Component 2 are Ni (moderate) and Co (weak) (Table 1.2). Strong and weak are relative terms; they help only in imparting some sense of order to the result of the PCA.

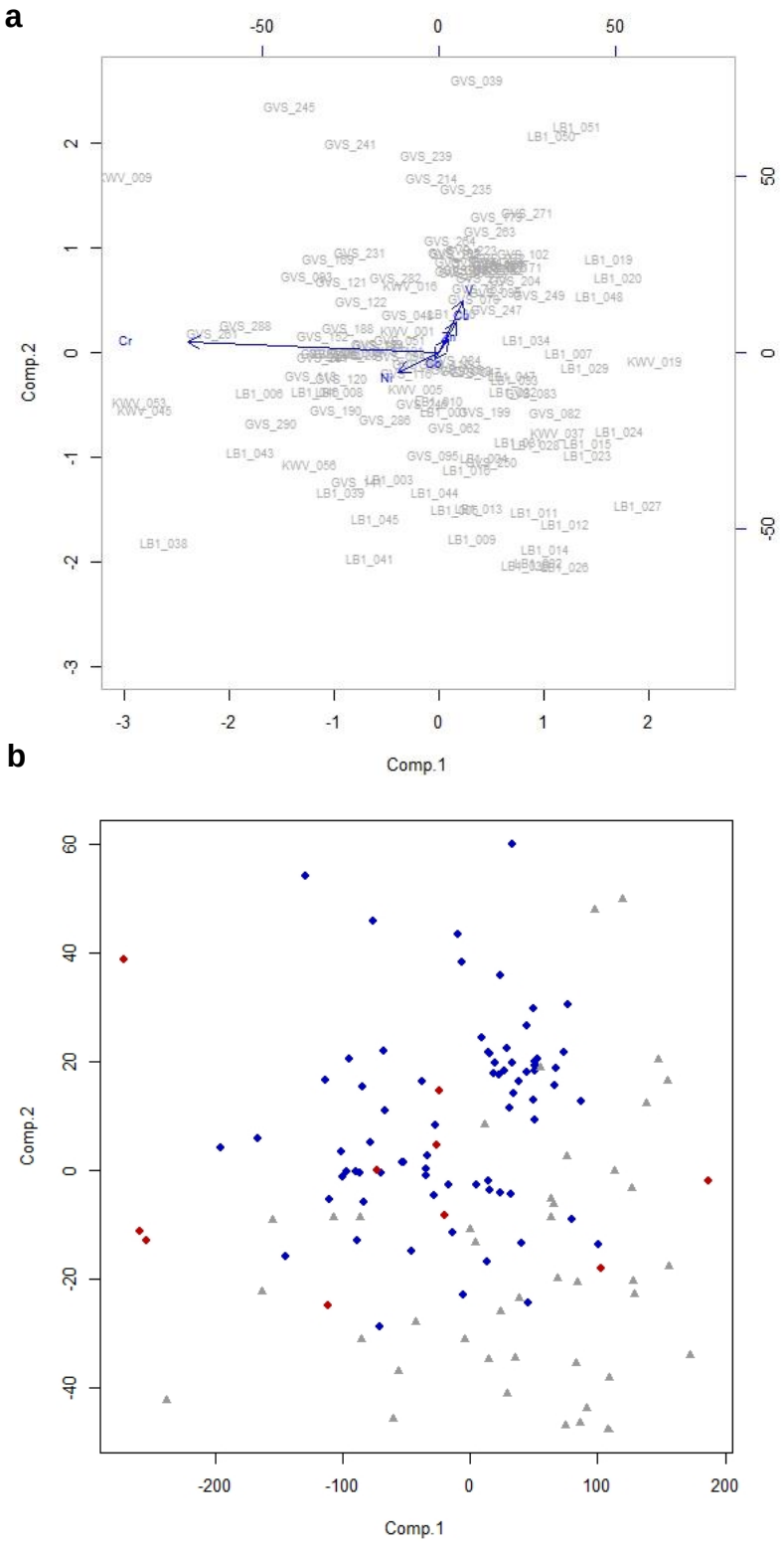

Figure 18: The top figure (18a) is the PCA of the transition metals Co, Cu, Cr, Ni, V, and Zn. The bottom figure (18b) shows the data as eigenvalues in a space defined by the two principal components. Data shown are GVS and KWV dolerites (blue and red circles, respectively), and Group 1 Lesotho basalts (grey triangles). A large degree of overlap between the dolerites and basalts may be observed. The GVS data and the KWV data overlap with each other.

Observing the variation due to the transition metals is a valuable intellectual exercise, even if these metals play no further part in this study. A PCA is an exploration of multivariate data to aid in establishing the presence of a latent system (assuming there is one) (Everitt & Hothorn, 2011). A PCA is designed to show variation so it will show variation; it is up to the interpreter of the PCA to decide on the relevance of the variation to the data and to what is being studied. Transition metals, although shown, are excluded from the geochemical analysis.

Table 1: Principal component analysis of the transition metals Co, Cu, Cr, Ni, V, and Zn. The importance of the components may be inferred from the proportion of variance. Generated with GCDkit.

	Comp. 1	Comp. 2	Comp. 3	Comp. 4	Comp. 5	Comp.6
Standard deviation	90.8587	23.1642	13.9659	8.81509	6.9035	3.9378
Proportion of variance	0.9044	0.05878	0.02136	0.008513	0.005221	0.001699
Cumulative proportion	0.9044	0.9631	0.9845	0.9931	0.9983	1.000

Table 2: Results table of the principal component analysis of the transition metals Co, Cu, Cr, Ni, V, and Zn. Generated with *R* and rounded to four significant figures. Empty cells denote negligible loadings *(Everitt & Hothorn, 2011)*.

	Comp. 1	**Comp. 2**	**Comp. 3**	**Comp. 4**	**Comp. 5**	**Comp. 6**
V	0,107	0,760		0,638		
Cr	-0,977	0,194				
Ni	-0,160	-0,434	-0,644	0,580		-0,155
Cu		0,367	-0,730	-0,442	0,360	
Co		-0,140	0,222	0,170	0,850	-0,424
Zn		0,205		-0,163	-0,371	-0,890

LIL and HFSE behaviour

The behaviour of LILs, HFSEs, and REEs (a subcategory of HFSE) should be more useful. The substitution of these metals for other cations in mafic melts places crystallographic lattices under strain and is thus energetically unfavourable. Therefore, LILs prefer the liquid phase over the solid phase. HFSEs, on the other hand, can only maintain charge balance if their respective crystallographic sites undergo coupled substitution. HFSEs have high ionic potentials, making them relatively insoluble in a melt and therefore relatively immobile during weathering, movement of hydrothermal fluids, or some other kind of metamorphism (White, 1999).

A major difference between the PCA of HFSEs and LILs (Fig. 19) and Figure 18 is the division in variance amongst the top three components. Table 1 describes most of the variation using only two components; Table 3 attributes variation to more components: Component 1 is attributing 61% to the total variation; Component 2 is attributing 31%; and Component 3 is attributing 4%. Together these components comprise around 96% of the total variation in the LILs (Ba, Rb, and Sr) and HFSEs (Zr and Nb) available in this dataset.

Sr is the only element with positive loadings on both components (Table 4) (moderate loading on Component 1 and strong loading on Component 2). Ba has a strong negative loading on Component 2 but has a moderate positive loading on Component 2. Zr has a moderate negative loading on Component 1 and a negligible loading on Component 2. Both Nb and Rb impart little variation with loadings only on components 3 (c. 4% of total variation) and 4 (c. 1% of total variation). Nb has a weak positive loading on Component 3 and a strong negative loading on Component 4. Rb has strong and weak negative loadings on components 3 and 4 respectively.

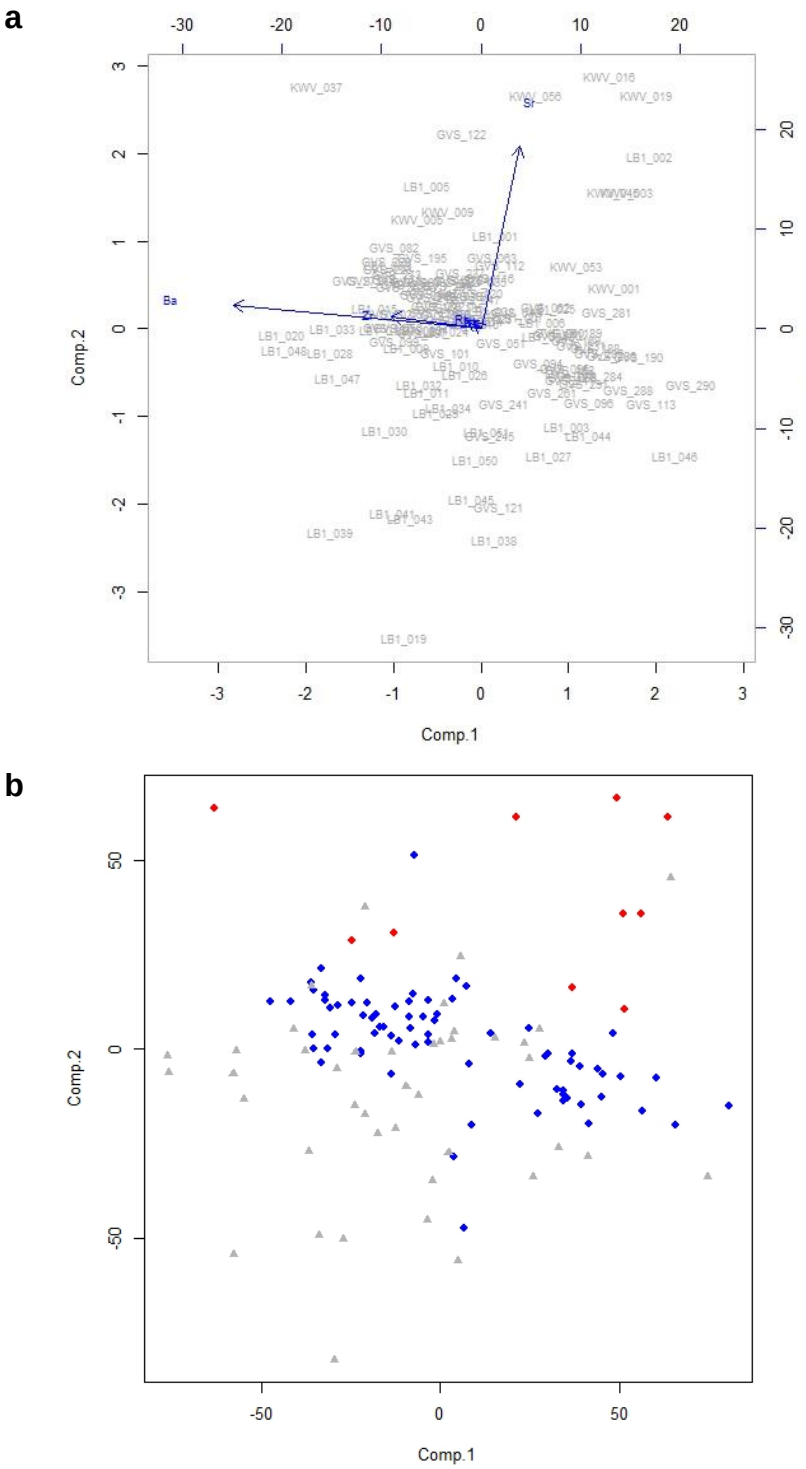

Figure 19: The top figure (19a) is a combined PCA of HFSEs (Nd and Zr) and LILs (Ba, Rb, and Sr). The bottom figure (19b) shows the data as eigenvalues in a space defined by the two principal components. Data shown are GVS and KWV dolerites (blue and red circles, respectively), and Group 1 Lesotho basalts (grey triangles). As with Figure 15 a large degree of overlap between the dolerites and basalts may be observed. The KWV data is not conformable to the rest of the data in 17b in contrast to Figure 15b where the KWV appears to be very conformable to one of the GVS clusters.

Table 3: Principal component analysis of the transition metals Co, Cu, Cr, Ni, V, and Zn. The importance of the components may be inferred from the proportion of variance. Generated with GCDkit.

	Comp. 1	Comp. 2	Comp. 3	Comp. 4	Comp. 5
Standard deviation	33.6240	23.1524	8.0358	4.3139	1.40788
Proportion of variance	0.6453	0.3059	0.03686	0.01062	0.001131
Cumulative proportion	0.6453	0.9513	0.9882	0.9988	1.000

Table 4: Results table of the principal component analysis of HFSEs (Nd and Zr) and LILs (Ba, Rb, and Sr). Generated with *R* and rounded to four significant figures. Empty cells denote negligible loadings *(Everitt & Hothorn, 2011)*.

	Comp. 1	Comp. 2	Comp. 3	Comp. 4	Comp. 5
Sr	0.374	0.926			
Zr	-0.303				
Ba	-0.875	0.364			
Nb			0.114	-0.991	
Rb			-0.992	-0.113	

Moving onto the REEs (Fig. 20), Component 1 is responsible for just over 96% of the total variation and Component 2 accounts for 3% of the total variation (Table 5). Y has a moderate positive loading on Component 1 and a strong positive loading on Component 2 (Table 6). Ce has a strong positive loading on Component 1 and a moderate negative loading on Component 2. Nd has a moderate positive loading on Component 1 and a negligible loading on Component 2. La has a moderate positive loading on Component 1 and a relatively weak negative loading on Component 2.

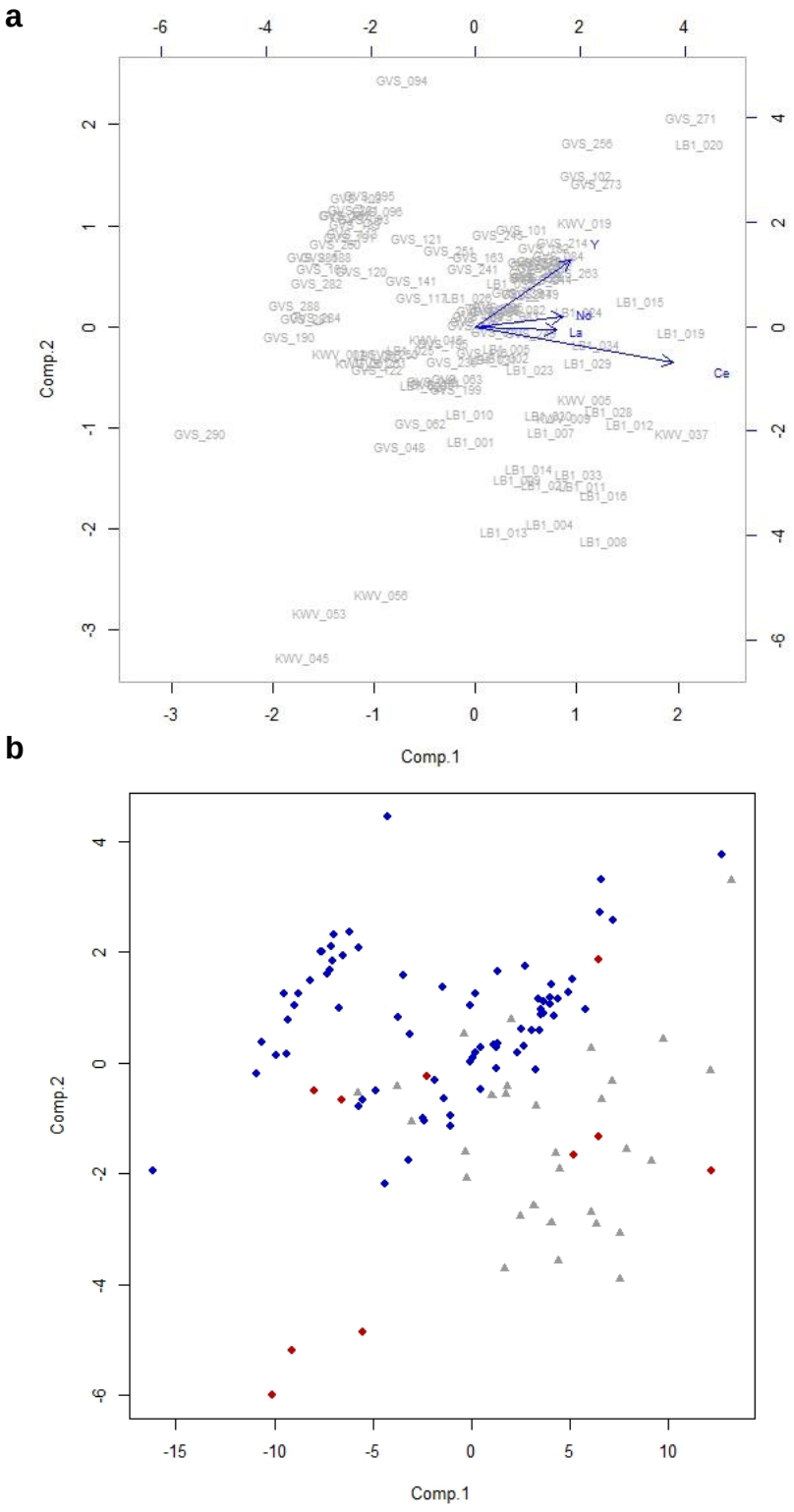

Figure 20: The top figure (20a) is a PCA of the REEs Ce, La, Nd, and Y. The bottom figure (20b) shows the data as eigenvalues in a space defined by the two principal components. Data shown are GVS and KWV dolerites (blue and red circles, respectively), and Group 1 Lesotho basalts (grey triangles). As with Figure 15, a large degree of overlap between the dolerites and basalts may be observed.

Table 5: Principal component analysis of the REEs Ce, La, Nd, and Y. The importance of the components may be inferred from the proportion of variance. Generated with GCDkit.

	Comp. 1	Comp. 2	Comp. 3	Comp. 4
Standard deviation	6.9367	1.2983	0.1744	0
Proportion of variance	0.9655	0.03382	0.0006108	0
Cumulative proportion	0.9655	0.9993	1.000	1

Table 6: Results table of the principal component analysis of the REEs Ce, La, Nd, and Y. Generated with *R* and rounded to four significant figures. Empty cells denote negligible loadings *(Everitt & Hothorn, 2011)*.

	Comp. 1	**Comp. 2**	**Comp. 3**	**Comp. 4**
Y	0.258	0.952	0.160	
Ce	0.868	-0.252		0.427
Nd	0.306		-0.725	-0.614
La	0.294	-0.162	0.670	-0.662

Enrichments in Cs, Rb, and K, and depletions in U, Ta, La, and Ce relative to the lower crust may be observed in Figure 21. Sr-Yb is compatible with the lower crust. The GVS (blue line) data is more variable and covers the spectrum between the KCA and UDS data and KWV data. This is not the case for U and Ta; the GVS data is the most depleted in these elements relative to the other Karoo data. There is a coalescence around Sr that, although mutual to all the data, shows that the KWV data is most enriched in Sr. This is followed by UDS, then KCA, and then GVS data. The GVS data has the most extreme dip in U content, and has the lowest enrichments of K, Nb, and Ta, and to a lesser extent, La, Ce, and Sr even though the peaks of these

elements are ruled by one GVS sample. The relative depletion in Ta recognized by Neumann et al. (2011) for the GVS dolerites is reflected in the KWV and UDS dolerites.

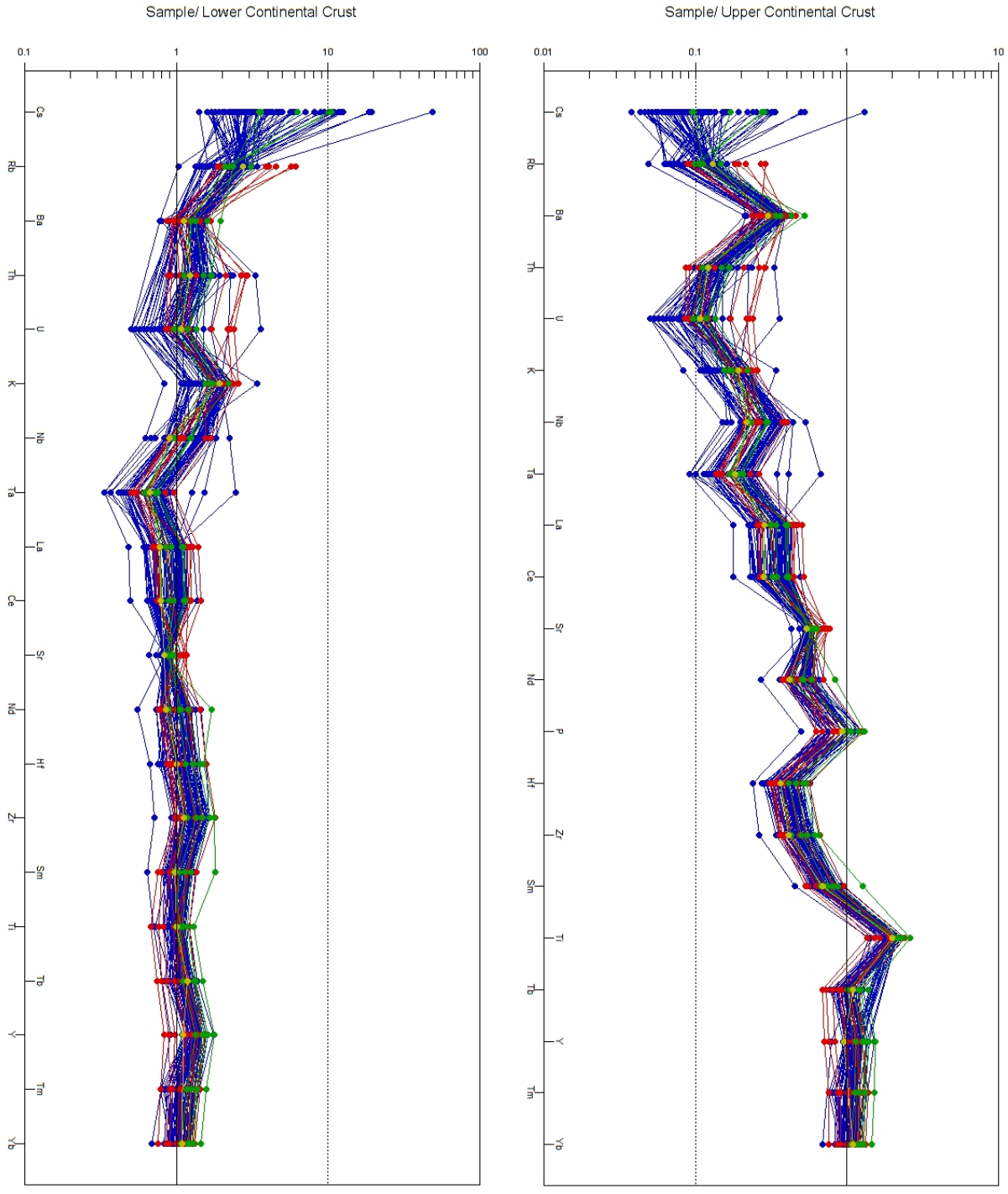

Figure 21: Spider plot normalized to the lower continental crust (21a; left) and upper continental crust (21b; right) after Taylor and McLennan (1995). Data shown are Karoo Central Area (**KCA; yellow**), Golden Valley Sill complex (**GVS; blue**), KWV Sill (**KWV; red**), and Underberg Dyke Swarm (**UDS; green**). The data is far more conformable to the lower continental crust than to the upper continental crust and is depleted relative to the upper continental crust.

Discussion

Representability of the study

This study is, in part, a review of data that was produced in five different laboratories. Utmost care was taken in upholding the integrity of the data for this reason. One possible consequence of this is that the data has been cleaned too much; i.e. too many data points have been removed because they were considered unrepresentative or outlying. However, due to the sensitivity of a PCA to igneous processes, it was felt important to look at only one rock type (as defined by SiO_2 content) as the presence of outliers would skew variation substantially. Since PCAs are used to look for hidden systematic relationships in multivariate data, it is important to remember that these data are derived from sills separated by many kilometres. Therefore, it must be acknowledged that some of the sampling locations may have underwent sill-specific processes that other sampling locations may not have. If this has occurred, this difference in igneous process should manifest itself as a systematic discrepancy between sampling locations.

A full suite of trace elements across all sampling locations would have been ideal, but this was not possible with the data available. As such, only trace elements common to all sampling locations were selected for analysis to make worthwhile comparisons and observations. Since petrologists have come to understand geological processes using trace elements, not having a full suite means that only a small part of a larger problem can be examined with this study. However, the data provides an E-W tract along 1500 km across the southern margins of the Karoo basin, which is considered sufficient to check for systematic variation.

The limited variation seen in this study should not, and cannot, be used to infer limited variation basin wide. Although a fair amount of distance is covered by this study (c. 1500 km), there is only one intrusive sampling location with more than 20 samples (GVS data) out of the five sampling locations. Also, sampling only occurred along the southern margins of the Karoo basin. This study does not utilize intrusive data sourced from the northern Karoo or from the Kaapvaal. The second largest intrusive population is the KWV data at 10 representable samples. There are numerous Lesotho basalts but these are included only as a control group against the behaviour of the dolerites.

The dataset compiled by this study seemingly samples a large area of the southern Karoo. A thorough examination of the integrity of the dataset used reveals that any extrapolations made by this study can only be applied to a much smaller area. The data is therefore enough and representable of the area that was sampled, yes, but not of the KLIP.

Implications of the findings

Major element chemistry is remarkably homogenous even within a small window of observation (Fig. 15). Most of the intrusive data is conformable to extrusive data (Fig. 16). The Na-poor group of Lesotho basalts are only conformable to the data in TiO_2, Al_2O_3, FeOt, and P_2O_5 space. The KWV data is consistently more SiO_2 poor than the GVS data and the UDS data seems to be more amenable to GVS data than to KWV data.

Sampling locations closer together were expected to have similar melt characteristics with geochemical discrepancies becoming more pronounced as distances increase between sampling locations. If this thinking were to hold then the UDS data would have to be closer to KWV data than to GVS data. Since this is clearly not the case then the implication is that spatial geochemical trends should not be based on major element chemistry.

Although a PCA cannot be used to quantify the data that is being processed, it does allow for metadata inferences. Normal basaltic data has considerable variation, as can be seen in Figure 22, in which data from several basaltic occurrences was analysed by PCA. However, in the case of the Karoo dolerites, there is little to no variation in trace element chemistry, with all the data overlapping to a greater or lesser extent. Figure 22 is a PCA that shows mafic material sampled from a variety of tectonic settings. What is important to note is the way the PCA has separated the data into two distinct populations as this could imply two distinct igneous processes (i.e. there could

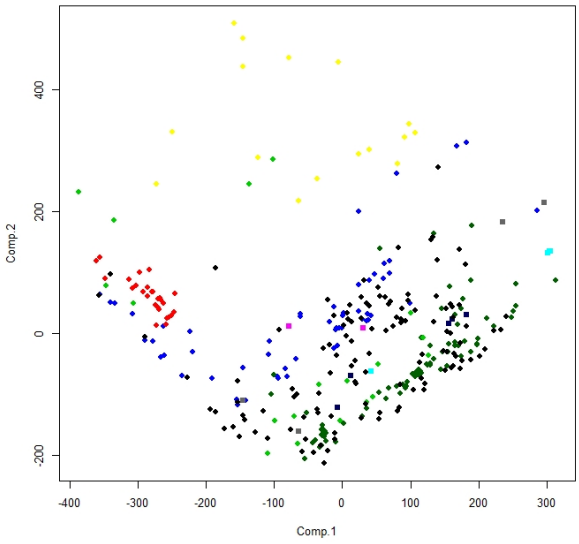

Figure 22: A PCA of mafic material sampled from a variety of tectonic settings shown as eigenvalues in a space defined by the two principal components.

be at least two petrological models at work in that dataset). It is important to note that the dataset used in this study is different from the dataset used to generate Figure 22.

The overlap of data from different sampling locations in the PCAs implies that the variation in LIL, HFSE, and REE chemistry could be linked systematically (i.e. petrologically). Therefore, spatial variation cannot be inferred from variation in trace element chemistry because there isn't enough variation to begin with. Trace element homogeneity could therefore be considered a product of some large-scale igneous process that was active throughout the Karoo basin c. 180 Ma. The data is remarkably compatible with the lower continental crust (Fig. 21 and has a faint low Ta subduction signature, like that found by Neumann et al. (2011). It should be noted that the control that Taylor and McLennan (1995) used for the lower continental crust is a residue due to the extraction of granodioritic upper crust and basaltic underplating.

The homogeneity is systematic, and therefore petrological across the sampling locations. However, a problem arises with accounting for the homogeneity. Homogeneity is derived from either high degrees of partial melting of a homogenous source or through thorough mixing between the parent melt and assimilated country rocks (i.e. contamination). It is possible that a high degree of partial melting of a common mantle source (not heterogeneous but not entirely homogenous either), mixing with assimilants/contaminants during ascent and intrusion, or the continued and wide-spread introduction of a common assimilant (Ecca and Beaufort rocks), could also result in large scale homogeneity. Neumann et al. (2011) estimates that the Karoo rocks are products of up to 10% assimilation of lower crust rocks and 60% fractional crystallization in the upper crust.

Logic and reason demands that the homogeneity be matched to a geological model. The Karoo magmas had to intrude the Karoo basin in some way. The western side of the basin is underlain by the basement rocks of the Natal-Namaqua Metamorphic Province (NNMP) and the eastern side of the basin is underlain by the Kaapvaal craton (Fig. 8). The NNMP is sutured to the Kaapvaal craton along a crustal scale discontinuity (Doringberg Fault). Another major discontinuity may be found in the Western Cape as the Heks River Fault. Only the Doringberg Fault intersects the upper mantle, according to seismic evidence (Tankard, et al., 2009).

These structures could be viable pathways for magma into the Karoo basin, but it is quite difficult to establish a source anywhere in the Karoo basin based on the

homogeneity in the trace elements. Ideally, variation would trend away from structures like the Doringberg Fault laterally and therefore spatially. Sampling locations closer to the Doringberg Fault would be more primitive, and sampling locations further from the Doringberg Fault would be more evolved if progressive differentiation occurs during magma travel before final emplacement.

However, trying to identify this spatially is arduous for a variety of reasons. The sampling location furthest from the Doringberg Fault is KCA, and it has one representable sample. The sampling location closest to the Doringberg Fault is UDS, and it has seven samples and not all the required trace elements. This leaves GVS and KWV sampling locations, which are separated by about 280 km (or less than 20% of the E-W tract covered by sampling locations) on Figure 12.

Using the sampling locations as proxies for spatial variation is unfeasible because of the meta-attributes of the data drawn from each location. Representability of spatial variation (if found) would be based on the integrity of the data. However, since the PCAs are not suggesting spatial variation, the integrity of the data does not have to be established. The homogeneity in the Karoo magmas conveniently side steps this issue.

The Karoo LIP as it stands now

Karoo magmatism is traditionally viewed either as a case of intraplate volcanism that is seemingly unrelated to arc volcanism or plume activity, or as the surficial manifestation of Karoo magmatism as a fingerprint of a prevailing geodynamic system. In each case, Karoo magmatism can be considered a product of some or other large-scale igneous system, and said large-scale igneous system can in turn be considered a result from the interplay between the upper mantle and mobile crust. Therefore, data needs to be representable of the KLIP and the KLIP needs to fit into what was going during the break-up of southern Gondwana.

Although the intention behind a model is to produce some measure of a universal answer, reality works differently. An igneous model is generated and tweaked according to the question that is being asked and relies greatly on the initial observation of the petrological environment of the igneous body. Without having a fundamental understanding of the petrological environment in which the model needs to be placed, the model itself will be a labour of love with no useable application (i.e. plume derived melts in the Karoo basin is not that far-fetched petrologically, but the

accepted and therefore expected physical manifestation of a plume is absent from the Karoo basin).

Although it is unfeasible to build a model that accounts for all observations and quirks in the data, any model for Karoo magmatism will have to account for fundamental observations. Before a model can be suggested, the homogeneity needs to be understood and the prevailing geodynamic environment leading up to the extrusion of the Karoo flood basalts needs to be determined. Something that can be said with some confidence is that the Karoo data does not seem to indicate widespread and continued contamination with a common assimilant.

Considering that the Karoo basin is underlain by NNMP basement rocks, the Karoo Supergroup sediments could be considered upper continental crust, and thus should not create a lower continental signature. Indeed, Luttinen (2018) attributed the Nb-poor province of the KLIP towards crustal contamination. However, a glance at the igneous data shows that the rocks are far more compatible with the lower continental crust (Fig. 22a) than to the upper continental crust (Fig 22b). The alternative to widespread contamination, large scale melting of a common subcontinental lithospheric mantle (SCLM) like that of Neumann et al. (2011), is much more alluring.

Karoo basin geodynamic environment

The Karoo basin can be thought of as a product of large-scale and incremental crustal subsidence as a by-product from induced mantle flow due to the continued subduction along the southern margin of Gondwana (Tankard, et al., 2009). Evidence for brittle failure exists in the Beaufort Group implying that the Cape Fold Belt was still deforming only tens of millions of years prior to the Karoo LIP (Hansma, et al., 2016). Both dextral (right handed) and sinistral (left handed) movement has been identified in the Cape Fold Belt (Andersen & Andreoli, 1990; Johnston, 2000; Blignault & Nicolaas, 2019). For this movement to be relevant, however, it needs to be coeval with late stage Karoo sedimentation (so upper Ecca at the oldest).

Spreading was starting c. 255 Ma in south-western Antarctica, as implied from ash fall in the Ecca Group which is derived from a reduced mantle source (McKay, et al., 2015). The Port Elizabeth Antitaxis is thought to be a product from the Falkland Islands driving the soft Cape Supergroup sediments up against the south-eastern margin of the NNMP (Johnston, 2000). The undeformed but coeval Natal Group sediments (Shone & Booth, 2005) imply that the Falkland Islands never made it that

far north; put another way, the Falkland Islands started to migrate west before it could deform the Natal Group sediments, but after moving eastward for long enough to deform Cape Supergroup sediments. This is a simplification but the important observation to make here is that there is evidence for a change in direction of tectonic movement along the southern margin of the Karoo basin.

The extrusion of the Karoo flood basalt province brought an end to the sedimentary infill of the Karoo basin, and the Stormberg depo-centre would have been the last depo-centre to subside before the KLIP. Therefore, it is important to understand what was going on around the Karoo basin c. 180 Ma because southern Gondwana broke up about this time and tectonic plates cannot move relative to one another if their movement cannot be accommodated by the surrounding tectonic plates.

Another reason why it is important to understand the prevailing geodynamic environment during the KLIP is because the Doringberg Fault is intimately involved in the geodynamics (Fig. 7). This predominantly strike-slip fault acts as the suture between the NNMP and Kaapvaal and has seen major movement along this plane. The Adelaide Subgroup is c. 4500 m thick west of the fault (NNMP basement) but barely 250 m thick east of the fault (Kaapvaal basement). Indeed, the fault displaced the Moho underneath South Africa by approximately 15 km (Tankard, et al., 2009).

Extension in western Antarctica, compression in the Cape Fold Belt and a change in direction of the Falkland Islands could be used to suggest large scale rotation. Although this study is not going to reconstruct the break-up of southern Gondwana, it is important to realize that the Doringberg Fault would have been exposed to major tectonic forces. Tankard et al. (2009) suggests that transpressive (oblique strike slip) forces would have been active on the Doringberg Fault. The relevance of this is that transpressive forces create regional but intense pressure gradients

If the Doringberg Fault is the source of Karoo magmatism and the Sterkspruit Complex is part of the vent complexes that produced the Karoo flood basalts then the plumbing system should be present in the underlying lithology. This assumes that the Stormberg sediments were still soft and squishy but contact metamorphism would have baked the sandstones into quartzites; the magma might just have punched right through as ponding and sill formation in quartzite is probably a lot harder than what it

sounds like. However, the lithostratigraphy of the Clarens Formation, the youngest member of the Stormberg Group, describes massive aeolian sandstones and not quartzites (not even quartzitic sandstones) (Bordy & Head, 2018). The upper Stormberg Group thus presents no evidence for thermal alteration. If the plumbing system is absent from the Stormberg Group then it could imply that the Drakensberg Group is not the focal point for the Karoo flood basalts.

Large scale tectonic movements aside, there was a latent basin-wide geodynamic environment in the Karoo basin. The Karoo basin can be considered as intracratonic, surrounded by rigid crustal blocks that are in turn hemmed in by neighbouring crustal blocks, and on it goes until one intersects a plate boundary. If the infill of the Karoo basin was controlled by the gradual subsidence of discrete crustal blocks as in Tankard et al. (2009) then it means that the state of stress in the surrounding and underlying crust would have been relaxed.

An arch only stays up because vertical compression is constantly being applied to it. A dome stays up because of similar mechanics but, if not secured to its foundations properly, will collapse all around its perimeter. Crustal blocks may flounder in a similar way if the inherited compression from surrounding crustal blocks is no longer sufficient to hold the blocks up. This could be a product of a large-scale change in the application and distribution of forces in the surrounding crustal blocks.

The latent geodynamic environment may be controlled by gravity (at least for the sedimentation of the Karoo basin). If one were to produce a cross section of the Karoo basin with the sills included, then the distribution of the sills could be used to determine a vertical state of stress in accordance with the gradual subsidence of the NNMP relative to the Kaapvaal as proposed by Tankard et al. (2009). Neumann et al. (2011) in fact shows this in their model of the GVS data (Fig. 21).

The implication of Coetzee & Kirsters (2017) is that the orientation, or spatial distribution, of the dykes cannot be used to infer a predominant crustal-scale stress regime as these dykes simply record sill-specific stresses at the time of emplacement. An interesting exercise would be to differentiate stand-alone dykes in the Karoo basin from dykes created during the propagation of sills as in Coetzee & Kirsters (2017) in the dykes shown in Figure 2.

The plume model for the Karoo

The dykes in the Karoo basin are emplaced in all directions (Fig. 2) and not in the expected radial dyke swarm that characterizes plume heads (Jourdan, et al., 2007b). Instead the Karoo Triple Junction (Fig. 1) has been postulated as the focal point of the mantle plume (Ernst & Buchan, 1997; Storey, et al., 2001). For the Karoo Triple Junction to be conformable to the KLIP, one would expect Jurassic-aged radiating dyke swarms; however, this is not the case.

Hastie et al. (2014) found that the orientation of the Karoo Triple Junction has more to do with inherited lithospheric structures from the Limpopo Belt than it does with a plume head. Although a plume could be placed underneath Mwenezi (Fig. 1), it will be discordant with surrounding dyke swarms as well as with the northern younging direction in the KLIP (Hastie, et al., 2014). Jourdan et al. (2006) stressed that Precambrian basement structures played a central role in controlling the orientations of Karoo-aged dykes. Dyke swarms in the Mwenezi-Sabi limb are either Proterozoic or Mesozoic in age (728-1683 Ma and 131-179 Ma, respectively) with dyke swarms in the Olifants River being Proterozoic (851-1713 Ma) and Archean (2470-2872 Ma) (Jourdan, et al., 2006).

Although this study is not attempting at undermining geological evidence for a plume, the observed homogeneity in the intrusive rocks is discordant with the variation expected of a plume as plumes do vary spatially (White, 2010). There are nephelinites and picrites in and around the midpoint of the Karoo Triple Junction (Cox, 1992; White, 1997). but the samples used in this study are more than 2000 km from the triple junction and extremely homogeneous.

It is very difficult to identify a single point of origin for the Karoo magmas in the Karoo basin using a plume model because of the high compatibility the magmas have with the lower crust (Fig. 21a). This implies that the tectonic regime during the emplacement of the KLIP may have been local to only the Karoo basin. Although an artefact of tectonic activity, the tectonic regime may have had nothing to do with the tectonic activity during the break-up of southern Gondwana and could imply that the Karoo triple junction and the breakup of Gondwana may not be related to the KLIP magmatism.

An interesting juxtaposition is between the plume model in explaining Karoo magmatism and the subsidence-driven sedimentation of the Karoo basin as according

to Tankard et al. (2009). A subtle contrast that has been drawn up is between the plume model and a planar feeder model. In the context of the Karoo, the plume model is mainly an attempt at explaining where the igneous material came from and how it was sourced. The planar feeder model, on the other hand, is an attempt at explaining where and how the igneous material entered the basin. The plume model is more of a chemical model, and the planar feeder model is more of a physical model. Any model that is proposed for the KLIP must be able to address chemical and physical problems as a unified model.

A model for intraplate magmatism

This study has determined that the GVS and KWV dolerites were created by a similar igneous process hence the homogeneity in trace elements. This process entails sourcing the melt, moving the melt, and ultimately the intrusion and extrusion of the melt as the Drakensberg Group, all within an intraplate setting. Trying to place the KLIP in an arc setting is just as difficult as trying to place it in a plume setting. There simply is no evidence for arc volcanism in the Cape Fold Belt (Tankard, et al., 2009).

Comparing the KLIP to other cases of intraplate igneous activity that is not related to arc or plume volcanism can prove to be an invaluable exercise. One such example is Mt Paektu (also known as Changbai Mountain, Figure 24), a volcano that sits on the border between China and North Korea. The volcano is c. 1000 km away from the nearest subduction zone (i.e. the Japanese volcanic arc chain) and there is no deep-seated thermal anomaly underneath it; only a hot mantle wedge (Tian, et al., 2016). Other than that, the volcanism has no links towards the Pacific Ring of Fire.

The volcanism of Mt Paektu (or rather, seismic activity) is a far-field product from the ongoing subduction in the north-western Pacific. Dehydration of the subducting slab generates the arc magmas that created modern day Japan and continuing subduction drives the subducting slab deeper into the mantle. The subducting slab eventually hits and is deflected along the boundary between the upper and lower mantle (Zhang, et al., 2015; Tian, et al., 2016). This conveyor belt means that not all the hydrated minerals are liberated underneath Japan and that there is a thick hot piece of mantle that is now sandwiched between modern crust and ancient crust (Zhao & Tian, 2013).

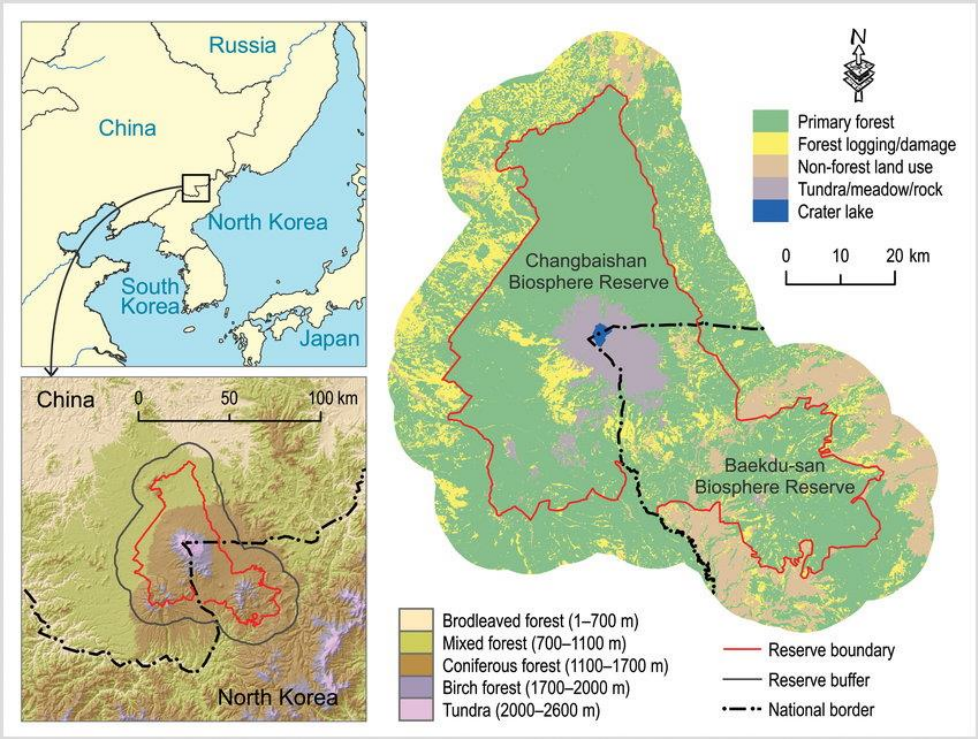

Figure 23: Map and inserts showing the location of Mt Peaktu *(Tang, et al., 2011)*.

Mt Paektu's volcanism is driven by secondary dehydration of ancient subducted crust. Seismic tomography backs this model up (the hot magma chamber is visible along with the dense subducted crust and upper and lower mantle) and seismic activity on Mt Paektu is deep, occurring at the point where the subducted crust is deflected along the boundary. The take home message from this example is that ancient subducted slabs can and does interact with the overlying mantle wedge long after initial subduction. Not only is this a far-field effect, but the magmatism can also manifest on surface (Zhao & Tian, 2013).

The comparison between the KLIP and Mt Paektu suggests a way to produce intraplate volcanism that is unrelated to arc or plume volcanism, and there are several physical similarities between the KLIP and Mt Paektu. Both cases are c. 1000 km away from the nearest subduction coeval with their emplacement/formation. Both cases cannot be reconciled with arc and plume models. Indeed, it is the very discrepancy between Mt Paektu and these models that led to the discovery of secondary dehydration of ancient subducted slabs underneath it. Mt Paektu is inadvertently a case of regional tectonics and the KLIP could similarly be a case of regional tectonics. It would be foolish to say that what is going underneath Mt Paektu today is what developed the KLIP. The Karoo magmas do have a faint subduction signature and the KLIP does not necessarily fit into an arc or plume model, but what Mt Paektu provides is a third model that is not only well understood, but accepted in literature.

Conclusion

Assessing the extent of the variation of trace elements in the Karoo data revealed two things. One, there is no real variation and the rocks are extremely homogeneous; and two, there are some pretty major issues with the data, even after the utmost care was taken in the construction of the dataset. The assessment of the geodynamic environment produced a suggestion that gravity could have facilitated the regional tectonic regime that expedited the KLIP. This model bears a noteworthy similarity to the subsidence-driven model for the sedimentation of the Karoo basin (Tankard, et al., 2009).

The KLIP is yet to be placed in a model that can account for most observations of it. However, before this can be done there is a host of other studies that needs to be done, such as determining the density structure of the upper mantle underneath South Africa from which invaluable thermal inferences can be made. Understanding how the subduction along the southern margin of Gondwana and the break-up of Gondwana affected the upper mantle underneath South Africa would shed light on the movement and interaction of ancient slabs and hot melts. These two studies alone will produce thought provoking results but should serve only to vet the representability of the KLIP to Mt Paektu's volcanism.

Of course, most of this can be a wild goose chase because of the extreme restrictions of applying observations and inferences from the sampling locations in this study to the whole of the KLIP. An easy remedy for this is a systematic and comprehensive sampling of exposed Drakensberg Group throughout the Karoo basin. Unfortunately, this would entail covering more than two thirds of the surface area of South Africa and be ludicrously expensive even before analyses are performed. This could be mitigated if access is granted to the relevant rocks from drill cores from the exploration wells in South Africa's juggernaut mining industry. However, this requires access to sensitive information and mines are not easily going to give up their cores or allow a third-party analysis of their cores.

Works Cited

Andersen, N. & Andreoli, M., 1990. The structural evolution of the coastal area between Danger Point and Struisbaai in the southern Cape Fold Belt, with implications for the siting of a nuclear power station. *South African Journal of Science,* 86(11), pp. 499-511.

Andersson, M. et al., 2013. Carbonatite ring-complexes explained by caldera-style volcanism. *Scientific Reports,* Volume 3, p. 1677.

Blignault, H. & Nicolaas, T., 2019. An Alternative Structural Model for the Development of the Cape Fold Belt Syntaxis and Groundwater Potential. *Earth Sciences,* 8(5), pp. 277-284.

Beniest, A., Koptev, A. & Burov, E., 2017. Numerical models for continental break-up: Implications for the South Atlantic. *Earth and Planetary Science Letters,* Volume 461, pp. 176-189.

Bordy, E. & Head, H., 2018. Lithostratigraphy of the Clarens Formation (Stormberg Group, Karoo Supergroup), South Africa. *South African Journal of Geology,* March, 121(1), pp. 119-130.

Bumby, A. & Guiraud, R., 2005. The geodynamic setting of the Phanerozoic basins of Africa. *Journal of African Earth Sciences,* Volume 43, pp. 1-12.

Campbell, I., 2006. Large Igneous Provinces and the Mantle Plume Hypothesis. *Elements,* Volume 1, pp. 265-269.

Catuneanu, O., 2004. Retroarc foreland systems—evolution through time. *Journal of African Earth Sciences,* Volume 38, pp. 225-242.

Catuneanu, O. et al., 2005. The Karoo basins of south-central Africa. *Journal of African Earth Sciences,* Volume 43, pp. 211-253.

Chevallier, L. & Woodford, A., 1999. Morpho-tectonics and mechanism of emplacement of the dolerite rings and sills of the western Karoo, South Africa. *South African Journal of Geology,* 102(1), pp. 43-54.

Coetzee, A. & Kirsters, A., 2017. Dyke-sill relationships in Karoo dolerites as indicators of propagation and emplacement processes of mafic magmas in the shallow crust. *Journal of Structural Geology,* Volume 97, pp. 172-188.

Coffin, M. & Eldholm, O., 1992. Volcanism and continental break-up: a global compilation of large igneous provinces.. *Geological Society Special Publications,* 68(1), pp. 17-30.

Cox, K., Bell, J. & Pankhurst, R., 1979. *The Interpretation of Igneous Rocks.* Dordrecht: Springer.

Cox, K., 1992. Karoo igneous activity, and the early stages of the break-up of Gondwana- land. In: A. Erlank, ed. *Magmatism and the causes of continental break-up.* s.l.:Geological Society of London Special Publications, pp. 37-148.

Duncan, A., 1987. The Karoo Igneous Province - a problem area for inferring tectonic setting from basalt geochemistry. *Journal of Volcanology and Geothermal Research,* Volume 32, pp. 13-34.

Duncan, R., Hooper, P., Marsh, J. & Duncan, A., 1997. The timing and duration of the Karoo igneousevent, southern Gondwana. *Journal of Geophysical Research,* 102(B8), pp. 18127-188.

Earth, G., 2020. *Sampling locations,* San Fransisco: Google.

Elliot, D., Fleming, T., Kyle, P. & Foland, K., 1999. Long-distance transport of magmas in the Jurassic Ferrar Large Igneous Province, Antarctica. *Earth and Planetary Science Letters,* Volume 167, pp. 89-104.

Elliot, D. & Fleming, T., 2000. Weddell triple junction: The principal focus of Ferrar and Karoo magmatism during initial breakup of Gondwana. *Geology,* 28(6), pp. 539-542.

Eriksson, P. et al., 2002. Late Archaean superplume events: a Kaapvaal–Pilbara perspective. *Journal of Geodynamics,* 34(2), pp. 207-247.

Ernst, R. & Buchan, K., 1997. Giant radiating dyke swarms: their use in identifying pre-Mesozoic large igneous provinces and mantle plumes. In: J. Mahoney & M. Coffin, eds. *Large Igneous Provinces: Continental, Oceanic, and Planetary Volcanism.* s.l.:AGU Geophysical Monographs, pp. 297-333.

Everitt, B. & Hothorn, T., 2011. *An Introduction to Applied Multivariate Analysis with R.* 1 ed. New York: Springer.

Feininger, T. & Seguin, M., 1983. Simple Bouguer gravity anomaly field and the inferred crustal structure of continental Ecuador. *Geology,* 11(1), pp. 40-44.

Floyd, P., 1985. Petrology and geochemistry of intraplate sheet-flow basalts, Nauru Basin, Deep Sea Drilling Project leg 89.. *Initial Reports of the Deep Sea Drilling Project, 89*, pp. 471-497.

Galerne, C., Neumann, E. & Planke, S., 2008. Emplacement mechanisms of sill complexes: Information from the geochemical architecture of the Golden Valley Sill Complex, South Africa.. *Journal of Volcanology and Geothermal Research,* Volume 177, pp. 424-440.

Galerne, C., Galland, O., Neumann, E. & Planke, S., 2011. 3D relationships between sills and their feeders: evidence from the Golden Valley Sill Complex (Karoo Basin) and experimental modelling. *Journal of Volcanology and Geothermal Research,* Volume 202, pp. 189-199.

Götz, A., Ruckwied, K. & Wheeler, A., 2018. Marine flooding surfaces recorded in Permian black shales and coal deposits of the Main Karoo Basin (South Africa): implications for basin dynamics and cross-basin correlation. *International Journal of Coal Geology,* Volume 190, pp. 178-190.

Greber, N. et al., 2020. New high precision U-Pb ages and Hf isotope data from the Karoo large igneous province; implications for pulsed magmatism and early Toarcian environmental perturbations. *Results in Geochemistry,* Volume 1, p. 100005.

Hansma, J. et al., 2016. The timing of the Cape Orogeny: New 40Ar/39Ar age constraints on deformation and cooling of the Cape Fold Belt, South Africa. *Gondwana Research,* Volume 32, pp. 122-137.

Hastie, W., Watkeys, M. & Aubourg, C., 2014. Magma flow in dyke swarms of the Karoo LIP: Implications for the mantle plume hypothesis. *Gondwana Research,* Volume 25, pp. 736-755.

Hawkesworth, C. et al., 1999. Mantle processes during Gondwana break-up and dispersal. *Journal of African Earth Sciences,* 28(1), pp. 239-261.

Hooper, P., Johnson, D. & Conrey, R., 1993. Major and trace element analyses of rocks and minerals by automated X-ray spectrometry. *Open File Report*, p. 37.

Janousek, V., Farrow, C. & Erban, V., 2006. Interpretation of Whole-rock Geochemical Data in Igneous Geochemistry: Introducing Geochemical Data Toolkit (GCDkit). *Journal of Petrology,* 47(6), pp. 1255-1259.

Johnson, M. et al., 1996. Stratigraphy of the Karoo Supergroup in southern Africa: an overview. *Journal of African Earth Sciences,* 23(1), pp. 3-15.

Johnson, M. et al., 1997. Chapter 12: The Foreland Karoo Basin, South Africa. In: R. Selley, ed. *Sedimentary Basins of the World.* Amsterdam: Elserivier, pp. 269-317.

Johnson, M. et al., 2006. Sedimentary rocks of the Karoo Supergroup. *The Geology of South Africa,* pp. 461-499.

Johnston, S., 2000. The Cape Fold Belt and Syntaxis and the rotated Falkland Islands: dexteral transpressional tectonics along the southwest margin of Gondwana. *Journal of African Earth Sciences,* 31(1), pp. 51-63.

Jourdan, F. et al., 2006. Basement control on dyke distribution in Large Igneous Provinces: case study of the Karoo triple junction. *Earth and Planetary Science Letters,* 241(1-2), pp. 307-322.

Jourdan , F. et al., 2007a. Distinct brief major events in the Karoo large igneous province clarified by new 40Ar/39Ar ages on the Lesotho basalts. *Lithos,* 98(1-4), pp. 195-209.

Jourdan, F. et al., 2007b. Major and Trace Element and Sr, Nd, Hf, and Pb Isotope Compositions of the Karoo Large Igneous Province, Botswana–Zimbabwe: Lithosphere vs Mantle Plume Contribution. *Journal of Petrology,* 48(6), pp. 1043-1077.

Le Bas, M., Le Maitre, R., Strekeisen, A. & Zanettin, B., 1986. A Chemical Classification of Volcanic Rocks Based on the Total Alkali-Silica Diagram. *Journal of Petrology,* 27(3), pp. 745-750.

Lindeque, A. et al., 2011. Deep Crustal Profile Across The Southern Karoo Basin And Beattie Magnetic Anomaly, South Africa: An Integrated Interpretation With Tectonic Implications. *South African Journal of Geology,* 114(3-4), pp. 265-292.

Luttinen, A., 2018. Bilateral geochemical asymmetry in the Karoo large igneous province. *Scientific Reports,* 8(5223).

Macdonald, J., 1989. Ring dyke. *Petrology.*

Malthe-Sørrenson, A., Planke, S., Svensen, H. & Jamtveit, B., 2004. Formation of saucer-shaped sills. *Physical Geology of High-Level Magmatic Systems,* Volume 234, pp. 215-227.

Marsh, B. & Phillip, J., 1996. Three dimensional magmatic filling of basement sill revealed by unusual crystal concen- trations. *Antarctic Journal of the United States,* Volume 31, pp. 39-40.

Marsh, J. et al., 1997. Stratigraphy and Age of Karoo Basalts of Lesotho and Implications for Correlations Within the Karoo Igneous Province. *Large Igneous Provinces: Continental, Oceanic, and Planetary Flood Volcanism,* Volume 100, pp. 274-272.

Mathieu, L., de Vries, B. v. W., Holohan, E. & Troll, V., 2008. Dykes, cups, saucers and sills: Analogue experiments on magma intrusion into brittle rocks. *Earth and Planetary Science Letters,* 271(1-4), pp. 1-13.

McClintock, M., Houghton, B., Skilling, I. & White, J., 2002. *The Volcaniclastic Opening Phase of Karoo Flood Basalt Volcanism: Drakensberg Formation, South Africa..* [Art] (American Geophysical Union Fall Meeting).

McKay, M. et al., 2015. Petrogenesis and provenance of distal volcanic tuffs from the Permian–Triassic Karoo Basin, South Africa: A window into a dissected magmatic province. *Geosphere,* 12(1), pp. 1-14.

McKenzie, D. & Bickle, M., 1988. The Volume and Composition of Melt Generated by Extension of the Lithosphere. *Journal of Petrology,* 29(3), pp. 625-679.

Middlemost, E., 1994. Naming materials in the magma/igneous rock system. *Earth-Science Reviews,* Volume 37, pp. 215-224.

Muirhead, J., Airoldi, G., White, J. & Rowland, J., 2014. Cracking the lid: Sill-fed dikes are the likely feeders of flood basalt eruptions. *Earth and Planetary Science Letters,* Volume 406, pp. 187-197.

Moulin, M. et al., 2011. An attempt to constrain the age, duration, and eruptive history of the Karoo flood basalt: Naude's Nek section (South Africa). *Journal of Geophysical Research,* Volume 116, p. B07403.

Moulin, M. et al., 2017. Eruptive history of the Karoo lava flows and their impact on early Jurassic environmental change. *Journal of Geophysical Research: Solid Earth,* 122(2), pp. 738-772.

Neumann, E., Svensen, H., Galerne, C. & Planke, S., 2011. Multistage Evolution of Dolerites in the Karoo Large Igneous Province, Central South Africa. *Journal of Petrology,* 52(5), pp. 959-984.

Ottley, C., Pearson, D. & Irvine, G., 2003. A routine method for the dissolution of geological samples for the analysis of EE and trace elements via ICP-MS. *Plasma Source Mass Spectrometry*, pp. 221-230.

Polteau, S. et al., 2008. Saucer-shaped intrusions: Occurrences, emplacement and implications. *Earth and Planetary Science Letters,* Volume 266, pp. 195-204.

Ramluckan, V., 1992. *The petrology and geochemistry of the Karoo sequence basaltic rocks in the Natal Drakensberg at Sani Pass.* Durban: University of Durban-Westville.

Ramsey, M. et al., 1995. An objective assessment of analytical method precision: comparison of ICP-AES and XRF for the analysis of silicate rocks. *Chemical Geology,* Volume 124, pp. 1-19.

Riley, T. et al., 2006. Overlap of Karoo and Ferrar Magma Types in KwaZulu-Natal, South Africa. *Journal of Petrology,* 47(3), pp. 541-566.

Roberts, R., Dixon, R. & Merkle, R., 2016. Distinguishing between legally and illegally produced gold in South Africa. *Journal of forensic science,* Volume 61, pp. S230-S236.

Sarbas & Baerbel, 2008. The GEOROC database as part of a growing geoinformatics network. *Geoinformatics 2008 - Data to Knowledge.*

Schoenberg, R. et al., 2003. The Source of the Great Dyke, Zimbabwe, and Its Tectonic Significance: Evidence from Re-Os Isotopes. *The Journal of Geology,* 111(5), pp. 565-578.

Selden, P. & Nudds, J., 2012. *Evolution of Fossil Ecosystems.* 2nd ed. s.l.:Elserivier.

Shone, R. & Booth, P., 2005. The Cape Basin: a review. *Journal of African Earth Sciences,* Volume 43, pp. 196-210.

Smith, R., Eriksson, P. & Botha, W., 1993. A review of the stratigaphy and sedimentary environments of the Karoo-aged basins of Southern Africa. *Journal of African Earth Sciences,* 16(1-2), pp. 143-169.

Storey, B., Leat, P. & Ferris, J., 2001. The location of mantle–plume centers during the initial stages of Gondwana breakup. In: R. Ernst & K. Buchan, eds. *Mantle plumes: their identification through time..* s.l.:s.n., pp. 71-80.

Storrie-Lombardi, M. & Fisk, M., 2004. Elemental abundance distributions in suboceanic basalt glass: evidence of biogenic alteration. *Geochemistry Geophysics Geosystems,* 5(10), pp. 1525-2027.

Svensen, H. et al., 2018. Gondwana Large Igneous Provinces: plate reconstructions, volcanic basins and sill volumes. *Large Igneous Provinces from Gondwana and Adjacent Regions,* Volume 463, pp. 17-40.

Svensen, H. et al., 2019. Thinking about LIPs: A brief history of ideas in Large igneous province research. *Tectonophysics,* Volume 760, pp. 229-251.

Sweeney, R. & Watkeys, M., 1990. A possible link between Mesozoic lithospheric architecture and Gondwana flood basalts. *Journal of African Earth Sciences (and the Middle East),* 10(4), pp. 707-716.

Tankard, A. et al., 2009. Tectonic evolution of the Cape and Karoo basins of South Africa. *Marine and Petroleum Geology,* Volume 26, pp. 1379-1412.

Tang, L., Li, A. & Shao, G., 2011. Landscape-level forest ecosystem conservation on Changbai Mountain, China and North Korea (DPRK). Mountain Research and Development. *Mountain Research and Development,* Volume 31, pp. 169-175.

Taylor, S. & McLennan, S., 1995. The geochemical evolution of the continental crust. *Reviews of Geophysics,* 33(2), pp. 241-265.

Thomson, K., 2004. Sill complex geometry and internal architecture: a 3D seismic perspective. *Physical Geology of High-Level Magmatic Systems,* Volume 234, pp. 229-232.

Thy, P. & Esbensen, K., 1993. Seafloor spreading and the ophiolitic sequences of the Troodos Complex: a principal component analysis of lava and dike compositions. *Journal of Geophysical Resarch,* 98(B7), pp. 11799-11805.

Tian, Y., Zhu, H., Zhao, D. & Liu, C., 2016. Mantle transition zone structure beneath the Changbai volcano: Insight into deep slab dehydration and hot upwelling near the 410-km discontinuity. *Journal of Geophysical Research: Solid Earth,* 121(8).

Ware, B. et al., 2018. Primary hydrous minerals from the Karoo LIP magmas: Evidence for a hydrated source component. *Earth and Planetary Science Letters,* Volume 503, pp. 181-193.

White, R., 1997. Mantle Plume origin for the Karoo and Ventersdorp Flood Basalts, South Africa. *South African Journal of Geology,* Volume 100, pp. 271-283.

White, W., 1999. *Chapter 7: Trace elements.* s.l.:Wiley.

White, W., 2010. Oceanic Island Basalts and Mantle Plumes: The Geochemical Perspective. *Annual Review of Earth and Planetary Sciences,* Volume 38, pp. 133-160.

Zhao, D. & Tian, Y., 2013. Changbai intraplate volcanism and deep earthquakes in East Asia: A possible link?. *Geophysical Journal International,* 195(2), pp. 706-724.

Zhang, M., Guo, Z., Cheng, Z. & Zhang, L., 2015. Late Cenozoic intraplate volcanism in Changbai volcanic field, on the border of China and North Korea: Insights into deep subduction of the Pacific slab and intraplate volcanism. *Journal of the Geological Society,* 172(5).

Ueki, K. & Iwamori, H., 2017. Geochemical differentiation processes for arc magma of the Sengan volcanic cluster, Northeastern Japan, constrained from principal component analysis. *Lithos,* Volume 290, pp. 60-75.